



**UNIVERSITEIT VAN PRETORIA
UNIVERSITY OF PRETORIA
YUNIBESITHI YA PRETORIA**

Title

**Important trace element concentrations in ovine liver as determined by energy
dispersive handheld X-ray fluorescence spectrometry**

by

Daniël Elhardus van Loggerenberg

**submitted in fulfilment of the requirements for the degree
MSc (Veterinary Science)**

in the

Faculty of Veterinary Sciences, University of Pretoria

Supervisor : Prof CJ Botha

Co-supervisor : Prof JG Myburgh

2016

TABLE OF CONTENTS

ACKNOWLEDGEMENTS.....	iii
DECLARATION.....	iv
LIST OF FIGURES.....	v
LIST OF TABLES.....	vii
LIST OF ABBREVIATIONS.....	viii
ABSTRACT.....	xi
CHAPTER 1: INTRODUCTION.....	1
CHAPTER 2: LITERATURE REVIEW.....	3
2.1 ESSENTIAL TRACE ELEMENTS IN VETERINARY SCIENCE.....	3
2.2 PHYSIOLOGICAL IMPORTANCE OF ESSENTIAL TRACE ELEMENTS.....	3
2.2.1 Copper.....	3
2.2.2 Iron.....	4
2.2.3 Manganese.....	6
2.2.4 Molybdenum.....	6
2.2.5 Selenium.....	6
2.2.6 Zinc.....	7
2.3 DEFICIENCIES AND TOXICOSES OF TRACE ELEMENTS IN SHEEP.....	8
2.3.1 Copper.....	8
2.3.2 Iron.....	10
2.3.3 Manganese.....	11
2.3.4 Molybdenum.....	11
2.3.5 Selenium.....	12
2.3.6 Zinc.....	13
2.4 SPECTROSCOPY AND SPECTROMETRY TECHNIQUES IN DETERMINING ESSENTIAL TRACE ELEMENT CONCENTRATIONS.....	13
2.4.1 Atomic Absorption Spectroscopy.....	13
2.4.2 Inductively Coupled Plasma Optical Emissions Spectrometry.....	15
2.4.3 Inductively Coupled Plasma Mass Spectrometry.....	19

2.5	X-RAY FLUORESCENCE SPECTROMETRY.....	22
2.6	HANDHELD X-RAY FLUORESCENCE SPECTROMETRY.....	26
2.7	AIM	28
2.8	OBJECTIVES.....	28
	CHAPTER 3: MATERIALS AND METHODS.....	29
3.1	EXPERIMENTAL DESIGN.....	29
3.1.1	Model System.....	29
3.1.2	Liver Samples.....	29
3.2	EXPERIMENTAL PROCEDURES.....	30
3.2.1	Preparation of Liver Samples for analysis.....	30
3.2.1.1	Preparation of liver samples for XRF spectrometry.....	30
3.2.1.2	Preparation of liver samples of ICP-MS analysis.....	35
3.2.2	Analysis of prepared Liver Samples.....	35
3.2.2.1	Handheld X-ray Fluorescence Spectrometry.....	35
3.2.2.2	ICP-MS analysis of Liver Samples performed by Reference Laboratory.....	43
	CHAPTER 4: RESULTS AND DISCUSSIONS.....	45
4.1	REFERENCE RANGES.....	45
4.2	PRECISION OF TOOLS (ICP-MS AND XRF) BY ELEMENT AND PREPARATION TYPE.....	49
4.2.1	Copper.....	49
4.2.2	Iron.....	50
4.2.3	Manganese.....	51
4.2.4	Molybdenum.....	52
4.2.5	Selenium.....	53
4.2.6	Zinc.....	54
4.3	CORRELATIONS.....	57
	CHAPTER 5: CONCLUSIONS.....	70
	REFERENCES.....	72
	APPENDUM A: ANIMAL ETHICS COMMITTEE APPROVAL.....	78

ACKNOWLEDGEMENTS

The following people are sincerely thanked for their help and support with this project:

Prof Christo Botha and Prof Jan Myburgh, my research supervisors, for their guidance, support and constant encouragement during difficult times, who have made this project possible.

Dr Pete Laver, for the statistical analysis.

Technical staff of the Pharmacology and Toxicology Laboratory, for their assistance.

Mrs Madelyn de Wet, for helping with layout and typing.

And last, but not least, my parents, who gave me everything and never thought it was enough.

DECLARATION

I, Dr Daniël Elhardus van Loggerenberg, declare that this Dissertation entitled: Important trace element concentrations in ovine liver as determined by energy dispersive handheld X-ray fluorescence spectrometry, which I herewith submit to the University of Pretoria in fulfilment of the requirements for the degree Magister Scientiae is my own original work, and has never been submitted for any academic award to any other institution of higher learning.

_____ **DATE** _____

LIST OF FIGURES

Figure 2.4.1	Atomic absorption spectroscopy block diagram.....	15
Figure 2.4.2	Different components of the plasma torch in ICP.....	17
Figure 2.4.3	Example of a circle polychromator.....	18
Figure 2.4.4	Layout of a typical ICP-OES instrument.....	19
Figure 2.4.5	Components of an ICP-MS instrument.....	20
Figure 2.4.6	Interface region of ICP-MS instrument.....	21
Figure 2.5.1	Components of an X-ray tube.....	23
Figure 2.5.2	Incident radiation causing X-ray fluorescence.....	24
Figure 2.5.3	Energy dispersive benchtop XRF spectrometer.....	25
Figure 2.6.1	Image of a handheld X-ray fluorescence spectrometer.....	27
Figure 3.2.1	Marked liver samples in drying oven.....	31
Figure 3.2.2	Mortar and pestle with oven dried sample.....	32
Figure 3.2.3	Vacuum sealed homogenous powder with vacuum sealer in background. Ethanol spray and mortar and pestle to the right of photo.....	32
Figure 3.2.4	Labcon muffle furnaces at Nutrilab laboratories.....	33
Figure 3.2.5	Crucibles with finished ash samples within muffle furnace...	34
Figure 3.2.6	Olympus Delta Premium 6000 XRF spectrometer in carry case.....	36
Figure 3.2.7	Olympus Delta XRF unit attached in an inverted position to the workstation with sample chamber.....	37
Figure 3.2.8	Laptop connected to workstation via USB cable.....	38
Figure 3.2.9	Mylar film roll and polyethylene sample cup (left). Stainless steel calibration coin in workstation's test chamber (right)....	38
Figure 3.2.10	Placing piece of Mylar film over sample cup (left). Placing polyethylene ring on top of Mylar film and securing film in place by pressing down on polyethylene ring (right).....	40
Figure 3.2.11	Finished sample cups after Mylar film has been secured and sample cups marked (left). Sample cup in inverted position in test chamber of Olympus workstation (right).....	40
Figure 3.2.12	Advanced Delta PC software with results.....	41

Figure 3.2.13	Dry ashed sample placed onto bottom piece of Mylar film to prevent sample from falling into sample cup (left). A second piece of Mylar film placed over sample to form an envelope (right).....	42
Figure 4.2.1	Cu concentrations as determined by ICP-MS and XRF.....	49
Figure 4.2.2	Fe concentrations as determined by ICP-MS and XRF.....	50
Figure 4.2.3	Mn concentrations as determined by ICP-MS and XRF.....	51
Figure 4.2.4	Mo concentrations as determined by ICP-MS and XRF.....	52
Figure 4.2.5	Se concentrations as determined by ICP-MS and XRF.....	53
Figure 4.2.6	Zn concentrations as determined by ICP-MS and XRF.....	54
Figure 4.3.1	Correlations between Cu concentrations determined by XRF spectrometry and ICP-MS.....	58
Figure 4.3.2	Correlations between Fe concentrations determined by XRF spectrometry and ICP-MS.....	60
Figure 4.3.3	Correlations between Mn concentrations determined by XRF spectrometry and ICP-MS.....	62
Figure 4.3.4	Correlations between Mo concentrations determined by XRF spectrometry and ICP-MS.....	64
Figure 4.3.5	Correlations between Se concentrations determined by XRF spectrometry and ICP-MS.....	66
Figure 4.3.6	Correlations between Zn concentrations determined by XRF spectrometry and ICP-MS.....	68

LIST OF TABLES

Table 2.3.1	Concentrations of copper in sheep liver.....	8
Table 2.3.2	Concentrations of iron in sheep liver.....	10
Table 2.3.3	Concentrations of manganese in sheep liver.....	11
Table 2.3.4	Concentrations of molybdenum in sheep liver.....	11
Table 2.3.5	Concentrations of selenium in sheep liver.....	12
Table 2.3.6	Concentrations of zinc in sheep liver.....	13
Table 4.1.1	Ranges of trace element concentrations (ppm) in ovine livers.....	45
Table 4.1.2	Concentrations of six trace elements (mg/kg(DW)) in the ovine liver (n=30) as determined by the reference laboratory (Nvirotek) using ICP-MS analysis.....	46
Table 4.1.3	Concentrations of six trace elements (ppm) in the ovine liver (n=30) as determined by handheld XRF analysis.....	46
Table 4.1.4	Ranges by order of magnitude.....	48
Table 4.2.1	ICP-MS median and range of intra-sample coefficient of variation (%) for element concentrations.....	56
Table 4.2.2	XRF median and range of intra-sample coefficient of variation (%) for element concentrations.....	56

LIST OF ABBREVIATIONS

AAS	Atomic absorption spectroscopy
Ag	Silver
As	Arsenic
ATP	Adenosine triphosphate
Bi	Bismuth
°C	Degrees Celsius
Ca	Calcium
Cd	Cadmium
Cl	Chlorine
cm	Centimetre
Co	Cobalt
CPU	Central processing unit
Cr	Chromium
Cu	Copper
Cu⁺	Copper(I)ion
Cu²⁺	Copper(II)ion
CV	Coefficient of variation
DA	Dry ashed
DAD	Dry ash duplicate
DW	Dry weight
e.g.	Exempli gratia
=	Equals
Fe	Iron
Fig	Figure
1st	First
g	Gram
h	Hour
H₀	Null hypothesis
H₁	Alternative hypothesis
Hg	Mercury
HNO₃	Nitric acid
HPDI	Highest posterior density interval
i.e.	Id est
ICP	Inductively coupled plasma
ICP-AES	Inductively coupled plasma atomic emission spectroscopy
ICP-MS	Inductively coupled plasma mass spectrometry
ICP-OES	Inductively coupled plasma optical emission spectrometry
K	Kelvin
K	Potassium
KV	Kilovolts
L	Laboratory
LCI	Lower confidence interval
LHPDI	Lower highest posterior density interval
Li-ion	Lithium ion
LOD	Limits of detection
max	Maximum
med	Median
MHz	Megahertz

min	Minimum
min	Minutes
µg/L	Microgram per litre
mg/L	Milligram per litre
mg/Kg	Milligram per kilogram
-	Minus
ml	Millilitre
mm	Millimetre
Mn	Manganese
Mo	Molybdenum
n	Sample size
Ni	Nickle
OD	Oven dried
ODD	Oven dried duplicate
OES	Optical emission spectrometry
P	Phosphorous
p-value	Calculated probability
Pb	Lead
%	Percentage
+	Plus
ppb	Parts per billion
ppm	Parts per million
ppt	Parts per trillion
r	Correlation coefficient
r²	Square of correlation coefficient
Rb	Rubidium
RF	Radio frequency
Rh	Rhodium
ROS	Reactive oxygen species
S	Sulphur
s	Seconds
Sb	Antimony
SD	Standard deviation
SDD	Silicon drift detector
2nd	Second
Se	Selenium
Si(Li)	Lithium drifted Silicon detector
Sn	Tin
Sr	Strontium
Th	Thorium
Ti	Titanium
U	Uranium
UCI	Upper confidence interval
UHPDI	Upper highest posterior density interval
USB	Universal serial bus
V	vanadium
v	Volts
W	Tungsten
WB	Wet blended
WBD	Wet blended duplicate

WW	Wet weight
XRF	X-ray fluorescence
Y	Yttrium
Z	Atomic number
Zn	Zinc
Zr	Zirconium

ABSTRACT

Trace elements are involved in a variety of biochemical processes essential to life and are required in minute amounts. There are no data available on the use of handheld X-ray fluorescence (XRF) spectrometry to determine concentrations of important trace elements in ovine livers. The aim of this study was to ascertain if the handheld X-ray fluorescence spectrometer will provide reliable concentrations of certain essential trace elements in the livers of sheep. Sheep livers (n=30) were obtained from abattoirs. Wet liver samples taken from 30 liver specimens were blended until homogeneity was achieved. An aliquot of the homogenised liver samples were oven dried at 50°C until a constant mass and were then pulverised using a mortar and pestle to obtain a fine powder. In addition, homogenised liver samples (n = 30) were also submitted for dry ashing. All the prepared liver samples (i.e. wet blended, oven dried and dry ashed) were then analysed using a handheld X-ray fluorescence spectrometer to determine concentrations of copper (Cu), iron (Fe), manganese (Mn), molybdenum (Mo), selenium (Se) and zinc (Zn). A reference laboratory analysed the same liver samples using ICP-MS to determine the concentrations of the above mentioned trace elements (control).

The means (mg/kg) of the ICP-MS results on a dry matter basis were: Cu (505), Fe (351), Mn (12.3), Mo (3.8), Se (1.8) and Zn (168). The means (mg/kg) of the XRF oven-dried results were: Cu (502), Fe (289), Mn (11.7), Mo (1.6) and Zn (141.9). Selenium could not be detected in oven-dried samples when using the XRF. The intra-sample coefficients of variation were similar between ICP-MS and XRF for oven dried samples for Cu, Fe and Zn and are within the same order of magnitude for all elements in dry ashed samples when comparing ICP-MS to XRF. However, the intra-sample coefficients of variation for Mn and Mo were approximately an order of magnitude larger using XRF. Although the precision for Se appears to be good when using XRF on dry ashed samples, Se was only detected in a few samples, so this value is not representative of the overall precision of XRF using the dry ashed preparation procedure for Se determination. Selenium was not detectable using XRF on wet blended and oven dried samples. The intra-sample coefficient of variation for Se was relatively high using ICP-MS,

suggesting that even the current 'gold standard' in detecting trace-elements may be imprecise in measuring Se. Overall, this suggests that the precision of sampling using XRF is relatively good for only Cu, Fe and Zn and relatively poor for Mn and Mo. Furthermore, XRF cannot be reliably used for measuring Se. Bayesian correlation were used to determine the best correlation between XRF and ICP-MS data. Bayesian correlation results are summarised by the median sample Pearson product-moment correlation coefficient (r), the 95% lower (LHPDI) and upper (UHPDI) highest posterior density intervals, the square of the sample correlation coefficient (r^2), and the probability that the correlation coefficient is positive. Overall, the oven-dried preparation procedure for XRF appeared to provide the best correlation with the ICP-MS data. For Cu and Zn these correlations were strong and the XRF method may represent a suitable substitute for ICP-MS. For Mn and Fe the correlations were moderately strong and the XRF method may be suitable depending upon the intended application. For Mo the correlation was moderate and XRF cannot be recommended. For Se no XRF method was suitable.

The advantage of handheld X-ray spectrometry is that the turnaround time of samples is reduced a great deal. Instead of submitting samples to a laboratory and waiting for results, samples can be analysed more rapidly with the use of a handheld X-ray fluorescence spectrometer.

CHAPTER 1

INTRODUCTION

In South Africa production animals are raised in different regions of the country. The grazing is unique to each region and varies tremendously depending on the climatic conditions in the area. Livestock is exposed to grazing that might be deficient in certain trace elements or grazing that might contain excess concentrations of trace elements. The Grootfontein Agricultural Development Institute situated near Middelburg, Eastern Cape Province, performed a survey of sheep and Angora goats raised in different grazing regions of South Africa (Hoon & Herselman, 2007). This survey identified regions that are deficient in certain trace elements as well as regions where flocks of sheep and goats might be prone to excessive intake of one or more trace elements. Apart from grazing that might contain high concentrations of certain trace elements, toxicities may also occur due to ingestion of supplementary feed or mineral formulations administered parentally in an attempt to treat or prevent deficiency states (McC Howell, 1996).

Certain trace elements are important to maintain physiological and biochemical processes in mammals. These minerals are referred to as essential trace elements (Van Doren, 2015) because of the important role they play in the health and well-being of mammals. It is important that veterinarians, livestock producers, feed manufacturers and agricultural scientists understand the role that essential trace elements play in the physiology of animals in order to ensure the health of the animals (Larson, 2005). Any imbalance in one or more of the essential trace elements may lead to poor growth and performance, reduced fertility, ill health and even mortalities (Reis *et al*, 2010). Thus, imbalances should be identified and corrected in order to prevent problems from occurring within any individual or group of animals. In order to identify imbalances of trace elements within an individual or a group of animals, certain diagnostic procedures are performed. These procedures may include clinical examinations, blood or serum analyses, organ biopsies or analyses of organ samples collected during post-mortem

examination or slaughter to determine concentrations of important trace elements (Kahn, 2005).

Spectroscopy and spectrometry have been used for decades to analyse and determine concentrations of important trace elements in animals. These techniques include atomic absorption spectroscopy, X-ray fluorescence spectrometry, inductively coupled plasma optical emission spectrometry and inductively coupled plasma mass spectrometry (Takahashi *et al*, 2000).

X-ray fluorescence spectrometers can be divided into wavelength dispersive (Helsen & Kuczumow, 2002) and energy dispersive spectrometers (Ellis, 2002). X-ray fluorescence instrumentation includes laboratory sized models as well as benchtop and handheld spectrometers.

Handheld X-ray fluorescence spectrometers are energy dispersive spectrometers (Beckhoff *et al*, 2006), which are small, portable and easy to transport. They have been used extensively in the disciplines of geology, mining, environmental science, forensics, arts and archaeology. Instead of transporting the samples to be analysed to a laboratory, handheld X-ray fluorescence spectrometers can be transported to where the samples are collected (Beckhoff *et al*, 2006).

There are no data available on the use of handheld X-ray fluorescence spectrometry to determine trace element concentrations in ovine livers or any other animal of veterinary importance. A gap therefore exists in the current knowledge about the use of handheld X-ray fluorescence spectrometers in the determination of important trace elements in veterinary diagnostics.

The aim of this research project was to ascertain if the handheld X-ray fluorescence spectrometer is a reliable diagnostic method to determine concentrations of certain essential trace elements, namely copper, iron, manganese, molybdenum, selenium and zinc, in the livers of sheep.

CHAPTER 2

LITERATURE REVIEW

2.1 ESSENTIAL TRACE ELEMENTS IN VETERINARY SCIENCE

Essential trace elements in the animal kingdom can be defined as chemical elements which are essential to the physiological well-being of the animal. These minerals are essential to normal health and function of animals and are required in minute amounts, defined as less than 1000 ppm dry weight (Van Doren, 2015).

For livestock producers, feed manufacturers, veterinarians and scientists the vital role that essential trace elements play in animal production and health is of the utmost importance (Larson, 2005). Some trace elements that play an important role in the physiological well-being of animals include copper, iron, manganese, molybdenum, selenium and zinc (Larson, 2005).

Essential trace elements can be described as having structural, electrolytic, catalytic or regulatory functions (Underwood & Shuttle, 1999). When the minerals form part of cytoskeletons in cells, the function is structural. By maintaining osmotic pressure within body fluids and tissues essential trace elements perform an electrolytic function. As part of metalloenzymes trace elements play a catalytic role within enzymatic and hormonal systems. Regulatory functions of essential trace elements include genetic transcription and hormonal function (Underwood & Shuttle, 1999).

2.2 PHYSIOLOGICAL IMPORTANCE OF ESSENTIAL TRACE ELEMENTS

2.2.1 COPPER

Copper (Cu) is a metal with atomic number (Z) 29 and standard atomic mass of 63.546 (Ebbing & Gammon, 1999). Copper is considered an essential trace element in biology.

In 1924 experiments involving rats indicated that copper played an important role in the synthesis of haemoglobin (McDonald *et al*, 2002). Due to the easy conversion of copper in its ionic states, Cu^+ and Cu^{2+} , it fulfils diverse roles in electron and oxygen transport within the body (Ebbing & Gammon, 1999). In all eukaryotes copper is essential in aerobic respiration (Mader, 2001).

Copper forms an important component of various proteins present in blood such as ceruloplasmin. Ceruloplasmin releases iron from mammalian cells into plasma which is then utilised for the synthesis of haemoglobin (McDonald *et al*, 2002). Erythrocyuprein is an important copper containing protein that occurs in red blood cells and plays a vital role in oxygen metabolism (Gartner & Weser, 1983). Of all the copper present in erythrocytes, 37% of the total copper concentration is present in erythrocyuprein (Gartner & Weser, 1983).

Cytochrome oxidase is another enzyme that contains copper and has enzymatic activity in oxidative phosphorylation (McDonald *et al*, 2002). Oxidative phosphorylation leads to the formation of adenosine triphosphate (ATP) which acts as a co-enzyme within cells for cellular metabolism (Mader, 2001). In addition, copper plays a vital role in the antioxidant system of mammalian cells by being a component of superoxide dismutase (Zhang *et al*, 2016). This antioxidant system protects cells against oxidative stress leading to free radicals that may damage cells and subsequent health problems. Copper is also involved in the pigmentation of hair, fur and wool. In sheep copper is required to produce good quality wool and is important in those breeds kept specifically for the production of wool for commercial use.

The main storage organ for copper in the body is considered to be the liver (Roberts & Sarkor, 2008). In sheep copper concentrations in the liver serves as a good indicator of the copper status.

2.2.2 IRON

Iron (Fe) is a metal with atomic number (Z) 26 and atomic mass of 55.845 (Ebbing & Gammon, 1999). By mass it is the most common element on earth.

In biology iron containing proteins are present in all living organisms. Of all the iron in mammalian tissues 90% or more is associated with proteins (McDonald *et al*, 2002). The most important of these iron containing proteins is haemoglobin. In the red blood cells of nearly all vertebrates the oxygen transport metalloprotein is haemoglobin. Haemoglobin is responsible for carrying oxygen from the lungs to the tissues of the rest of the body (Mader, 2001).

In serum, iron is present as transferrin, a glycoprotein that binds iron tightly, but reversibly. Transferrin controls the concentration of free iron in biological fluids and is involved in the transport of iron in the body (Elsayed, Sharif & Stack, 2016). The liver is the main organ where transferrin is synthesised (Morton & Tavill, 1977).

Ferritin is an iron containing protein providing a form of storage for iron. Ferritin is present in the bone marrow, kidney, liver and spleen (Mader, 2001). Free iron is toxic to cells as it acts as a catalyst in the formation of free radicals from chemically reactive oxygen species (ROS) (Mader, 2001). Ferritin stores iron in a non-toxic form (Mader, 2001).

Another iron containing protein serving as an iron storage complex is haemosiderin. Haemosiderin is only found within cells and do not circulate in blood. As opposed to ferritin, the iron in haemosiderin is poorly available to areas within the body where iron is required. Haemosiderin deposits are limited in normal animals. Due to the toxic nature of free iron within the body, haemosiderin is a protective mechanism to contain free iron (McDonald *et al*, 2002).

Iron plays an important role in a number of biochemical reactions. Iron is part of the enzymes (cytochromes) associated with the electron transport chain (Mader, 2001) (Warren & Smith, 2009). The processes involved in the electron transport chain eventually lead to the production of ATP, an important store for energy in cells (Mader, 2001). The oxidation and reduction activity of bound iron facilitates the transportation of electrons.

2.2.3 MANGANESE

Manganese (Mn) is a metal with atomic number (Z) 25 and atomic mass of 54.938 (Ebbing & Gammon, 1999).

Concentrations of manganese in mammalian tissues are very low (McDonald *et al*, 2002). The liver, skeleton, kidneys, pancreas and pituitary gland contains the highest concentrations of manganese (McDonald *et al*, 2001). Manganese is stored mainly in bone with the remainder mostly concentrated in the liver and kidneys. In adult sheep, the soft tissue that contains the highest Mn concentration is the liver (Underwood & Shuttle, 1999). In biology, manganese ions function as cofactors to enzymes and serves as an activator of many enzymes for example kinases and hydrolases. Some of the manganese containing enzymes are vital in the detoxification of superoxide free radicals.

2.2.4 MOLYBDENUM

Molybdenum (Mo) is a metal with atomic number (Z) 42 and atomic mass of 95.95 (Ebbing & Gammon, 1999).

In biology molybdenum forms part of a wide array of cofactor enzymes and is thus regarded as trace element essential for life in all higher eukaryote organisms. In 1953 it was discovered that xanthine oxidase, an important enzyme in purine metabolism, is a molybdenum containing metalloenzyme (McDonald *et al*, 2002). This was the first indication of an essential metabolic role for molybdenum. Molybdenum is also part of aldehyde oxidase and sulphite oxidase (Mader, 2001). Aldehyde oxidase is located in the cytosolic compartment of cells and is a metabolising enzyme. Sulphite oxidase is an enzyme that plays an important role in the cascade leading to the formation of ATP in oxidative phosphorylation (Mader, 2001). An important interaction of molybdenum with sulphide is the formation of thiomolybdates which inhibits the biochemical effectiveness of copper (Goodrich & Tillman, 1966).

2.2.5 SELENIUM

Selenium (Se) is a non-metal with atomic number (Z) 34 and atomic mass of 78.971 (Ebbing & Gammon, 1999).

During the 1950's supplementation of sheep and cattle diets with selenium demonstrated that most myopathies occurring in sheep and cattle can be prevented (McDonald *et al*, 2002). It was concluded that selenium is of nutritional importance and selenium became recognised as an essential trace element. In 1973 it was reported that selenium forms part of glutathione peroxidase (McDonald *et al*, 2002), an enzyme responsible for the catalytic reaction to remove hydrogen peroxide, thus protecting the body's cellular membranes from oxidative damage (Carlson *et al*, 2016). The structure of glutathione peroxidase contains four selenium atoms. After vitamin E, glutathione peroxidase forms a second line of defence in protecting the body from free radicals. Even if vitamin E levels are adequate some free radicals still remain and glutathione peroxidase can remove these harmful molecules. Glutathione peroxidase thus has a sparing effect on vitamin E. Vitamin E is required to maintain lipid membrane integrity and glutathione peroxidase reduces the amount of vitamin E needed for this function (Carlson *et al*, 2016). Selenium, as part of glutathione peroxidase, and vitamin E has a mutual beneficial effect on the functions and concentrations of each other.

Selenium plays an important role in the function of the thyroid gland (McDonald *et al*, 2002). This is due to the fact that selenium participates as a cofactor in three of the four known types of thyroid hormone deiodinases (McDonald *et al*, 2002). The thyroid hormone deiodinases activate and deactivate various thyroid hormones and their metabolites. In sheep type I deiodinase is present in the liver and kidneys (McDonald *et al*, 2002).

2.2.6 ZINC

Zinc (Zn) is a metal with atomic number (Z) 30 and atomic mass of 65.38 (Ebbing & Gammon, 1999).

As an essential trace element zinc is widely distributed throughout mammalian tissues (McDonald *et al*, 2002). Zinc is present in nearly a hundred specific enzymes, such as carbonic anhydrase, lactate dehydrogenase, alkaline phosphatase, pancreatic carboxypeptidase and glutamic dehydrogenase (Swenson & Reece, 1993). Carbonic anhydrase serves an important function in the transportation of carbon dioxide out of tissues. In transcription factors,

proteins involved in gene expression, zinc serves as structural ions (Mader, 2001). The storage and transport of zinc takes place in the form of metallothioneins. Zinc primarily accumulates in bones, but some is also stored in the liver.

2.3 DEFICIENCIES AND TOXICOSES OF TRACE ELEMENTS IN SHEEP

The deficiencies and toxicities of six important trace elements of sheep, evaluated in this study, will be reviewed briefly. These essential trace elements include copper, iron, manganese, molybdenum, selenium and zinc. All of these are present in the livers of sheep and the concentrations of these trace elements can be determined by various analytical techniques.

2.3.1 COPPER

Table 2.3.1 Concentrations of copper in sheep liver as listed in *Mineral levels in Animal Health* (Puls, 1994).

Deficient	0.5 – 4.0 ppm wet weight
Adequate	25 – 100 ppm wet weight
Toxic	250 – 1000 ppm wet weight

Copper deficiency

Two main causes of copper deficiency in sheep are copper-deficient soils and excessive supplementation of feed with molybdenum and sulphur (Erickson, 2015). Pastures cultivated in copper-deficient soils provides insufficient copper in the grazing for sheep during spring and it is therefore important to supplement deficient soils with a copper containing fertiliser. Molybdenum-sulphur compounds (thiomolybdates) are formed in the rumen which may complex with proteins and copper and lead to signs of copper deficiency (Dezfoulian *et al*, 2012) as these thiomolybdates thus inhibits absorption of dietary copper (McDonald *et al*, 2002). When thiomolybdates enters the bloodstream systemic copper metabolism are also affected leading to further signs of copper deficiency.

Excessive fertilisation of crops with molybdenum fertilisers may also result in copper deficiency.

Copper deficiency occurs in both lambs and adult sheep, the most important being enzootic ataxia or swayback in lambs (McDonald *et al*, 2002). Clinical signs may be present at birth or between 1 - 6 months of age. Typical of enzootic ataxia is the inability of the lamb to stand or an uncoordinated gait. When pregnant ewes ingest insufficient copper, foetal development is impaired thus leading to the onset of enzootic ataxia or swayback in newborn and young lambs.

One of the most prominent manifestations of copper deficiency in adult sheep is the absence of crimp in the wool. Copper forms part of an enzyme which plays an important role in the formation of bridges between protein molecules within the wool fibre (McDonald *et al*, 2002). Without the formation of these protein bridges the wool will be lacking crimp.

Copper poisoning

Copper poisoning in sheep is very important as they are highly susceptible to copper toxicosis (Menzies *et al*, 2003). Copper poisoning can be classified as acute or chronic copper poisoning.

Acute copper poisoning is rare. The onset of acute copper poisoning occurs after ingestion of excessive amounts of copper in a short period of time. One of the most common causes of acute copper poisoning is excessive dosing of sheep with copper sulphate for medicinal or prophylactic purposes (Bath & de Wet, 2000). Signs of acute copper poisoning include depression, abdominal pain, blue-greenish diarrhoea, hypothermia, tachycardia, ataxia, paralysis and death (Reis *et al*, 2010).

Chronic copper poisoning is common in South Africa among sheep. Ingestion of subtoxic doses of copper over a prolonged period of time causes gradual accumulation of copper in the liver and after a stressful incident copper is released and causes a severe haemolysis. Regions in South Africa that are very prone to chronic copper poisoning among sheep flocks include the Karoo and the southern Free State (Hoon & Herselman, 2007). This form of chronic copper

poisoning that occurs among sheep within these regions are also called enzootic icterus (Bath & de Wet, 2000). In the Karoo and southern Free State regions copper concentrations in some of the vegetation is at such an elevated concentration that it results in accumulation in the ovine liver and chronic copper poisoning regularly occurs among sheep flocks in this region (Boyazoglu, 1973).

Chronic copper poisoning can be classified into a pre-haemolytic phase and a haemolytic phase (Sansinanea *et al*, 1996). During the pre-haemolytic phase copper accumulates within the liver and the animal exhibits no clinical signs. Due to the systematic accumulation of copper in the liver, single cell necrosis of hepatocytes occurs (Reis *et al*, 2010). The haemolytic phase is precipitated by a sudden release of the accumulated copper within the liver which spills into the bloodstream. This is then followed by clinical signs such as icterus, anaemia, anorexia, ruminal stasis, haemoglobinuria and death (Bath & de Wet, 2000). A typical post-mortem finding in sheep that died from chronic copper poisoning is dark pigmented or black kidneys (Bath & de Wet, 2000).

2.3.2 IRON

Table 2.3.2 Concentrations of iron in sheep liver as listed in *Mineral levels in Animal Health* (Puls, 1994).

Deficient	15-25 ppm wet weight
Adequate	30-300 ppm wet weight

Iron deficiency

In grazing sheep iron deficiency is very rare (Kahn, 2005). Anaemia may occur in lambs that are housed and do not have access to soil (Vatn & Framstad, 2000). Oral or injectable iron supplementation is administered to prevent iron deficiency anaemia in housed lambs (Vatn & Framstad, 2000).

Iron toxicosis

Iron toxicosis is very rare in sheep (McDonald *et al*, 2002). It can occur with prolonged oral administration of the element and results in gastrointestinal disturbances (McDonald *et al*, 2002).

2.3.3 MANGANESE

Table 2.3.3 Concentrations of manganese in sheep liver as listed in *Mineral levels in Animal Health* (Puls, 1994).

Deficient	1.0 - 2.1 ppm wet weight
Adequate	2.0 – 4.4 ppm wet weight
Toxic	5.0 – 380 ppm wet weight

Manganese deficiency

Deficiency of manganese in grazing sheep is rare. Signs of acute deficiency include skeletal abnormalities, ataxia in newborn lambs and reproductive failure (McDonald *et al*, 2002).

Manganese toxicosis

Even at high concentrations manganese is low in toxicity (Bath & de Wet, 2000).

2.3.4 MOLYBDENUM

Table 2.3.4 Concentrations of molybdenum in sheep liver as listed in *Mineral levels in Animal Health* (Puls, 1994).

Normal	1.5 – 6.0 ppm dry weight
Toxic	30 – 60 ppm dry weight

Molybdenum toxicosis

High levels of molybdenum in the diet lead to the formation of thiomolybdates that complex copper and induces copper deficiency in sheep (McDonald *et al*, 2002).

2.3.5 SELENIUM

Table 2.3.5 Concentrations of selenium in sheep liver as listed in *Mineral levels in Animal Health* (Puls, 1994).

Deficient	0.01 – 0.10 ppm wet weight
Adequate	0.25 – 1.5 ppm wet weight
Toxic	15.0 – 30.0 ppm wet weight

Selenium deficiency

In South Africa low soil selenium concentrations are especially encountered in the coastal regions of the Eastern and Western Cape provinces (Van Ryssen, 2001) although it may also occur in other parts of South Africa as well (Van Ryssen, 2001). Pastures may become deficient in selenium when excessive amounts of superphosphate fertiliser is used (Bath & de Wet, 2000). Lush clover pastures may also lead to selenium deficiency (Bath & de Wet, 2000).

Selenium deficiency is sometimes associated with deficiencies of vitamin E. White muscle disease is caused when there is a deficiency in both selenium and vitamin E. Myocardial lesions can cause sudden death in lambs (Erickson, 2015).

Other non-specific signs associated with selenium deficiency include a reduced immune response, poor growth in young animals and poor fertility among breeding animals.

Selenium toxicosis

Chronic selenium toxicosis may occur when sheep graze selenium containing plants which accumulate selenium from high seleniferous soils (Van Ryssen, 2001). In areas with low annual rainfall and alkaline soil the bioavailability of selenium for selenium-accumulating plants increases. Chronic selenium toxicosis manifests as lethargy, joint stiffness and weakening of claws and hooves.

Acute selenium toxicosis occurs when large amounts of selenium are ingested within a short period of time. Incorrect dietary supplements or parenteral administration of selenium containing formulations may lead to the acute form of

toxicosis. Acute toxicosis may cause death mainly due to respiratory failure (McDonald *et al*, 2002).

2.3.6 ZINC

Table 2.3.6 Concentrations of zinc in sheep liver as listed in *Mineral levels in Animal Health* (Puls, 1994).

Deficient	20 – 30 ppm wet weight
Adequate	30 – 75 ppm wet weight
Toxic	>400 ppm wet weight

Zinc deficiency

Grazing or feed deficient in zinc may lead to signs of zinc deficiency in livestock (Bath & de Wet, 2000). Signs of zinc deficiency in sheep include loss of wool, decreased spermatozoal production and a weakened immune system (Bath & de Wet, 2000).

Zinc toxicosis

Zinc toxicosis is rare among sheep (Bath & de Wet, 2000).

2.4 SPECTROSCOPY AND SPECTROMETRY TECHNIQUES IN DETERMINING ESSENTIAL TRACE ELEMENT CONCENTRATIONS

2.4.1 ATOMIC ABSORPTION SPECTROSCOPY

Atomic absorption spectroscopy (AAS) was first described as an analytical method to quantitatively determine chemical elements by Gustav Robert Kirchhoff, a physicist, and Robert Wilhelm Bunsen, a chemist, in the second half of the 19th century (Kairtyahann, 1980). Both Kirchhoff and Bunsen were scientists at the University of Heidelberg, Germany. The Bunsen burner, invented by Robert Bunsen, formed an integral part of their apparatus to analyse chemical elements.

During the early 1950s the modern form of AAS was developed by a team of Australian chemists led by a British/Australian physicist Sir Alan Walsh (Fuwa, 1999). Sir Alan Walsh's article "The Application of Atomic Absorption Spectra to Chemical Analysis" was published in 1955 (Walsh, 1989) and is considered a pivotal article on trace element analysis. The modern form of AAS uses the absorption of optical radiation by free atoms in the gaseous state therefore allowing the quantitative determination of different chemical elements.

To analyse a sample in order to determine its atomic constituents, atomisation of the sample has to take place. AAS currently uses two types of atomisers, namely flame and electrothermal atomisers (Robinson, 1996). Flame atomisers are the oldest atomisers used. Electrothermal atomisers have a lower limit of detection than flame atomisers and thus detects trace elements at much lower concentrations than flame atomisers (Kryazhov *et al*, 2014). In a study conducted in 2005, bovine liver samples were analysed using both a flame atomiser AAS and an electrothermal atomiser AAS to determine copper and zinc concentrations (Nomura *et al*, 2005). The electrothermal atomiser method proved to be more reliable in determining the concentrations of copper and zinc when compared to the flame atomiser method (Nomura *et al*, 2005).

After a sample passes through the atomiser, the atoms produced are then irradiated by optical radiation (Robinson, 1996). The radiation source can be a continuum radiation source or could be an element specific radiation source (Robinson, 1996). After irradiation of atoms a monochromator is used to separate specific radiation associated with an element or elements within the sample being analysed. The monochromator corresponds to a certain spectral bandwidth and can be described as a wavelength selector of some sort (Eskina *et al*, 2016). In physics the term monochromatic refers to a single wavelength (Giancoli, 1998). After passing through the monochromator the element specific radiation separated by the monochromator reaches a detector which in turn measures the incoming radiation (Robinson, 1996).

The following block diagram illustrates the basic components of an AAS apparatus.

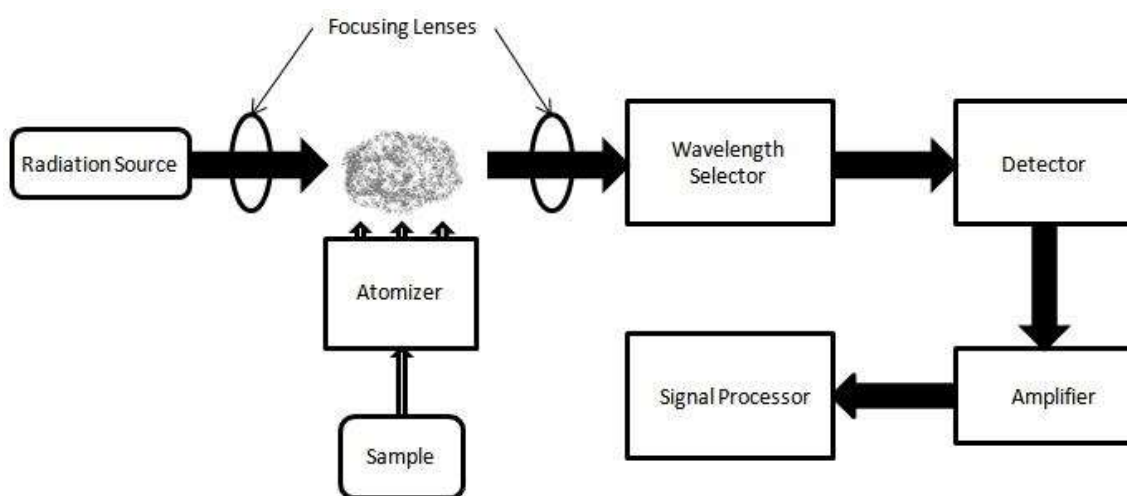


Figure 2.4.1 Atomic absorption spectroscopy block diagram

(https://en.m.wikipedia.org/wiki/Atomic_absorption_spectroscopy, accessed 05/06/2016).

AAS has been used for decades in various scientific disciplines such as toxicology, biophysics and pharmacology to determine concentrations of chemical elements in solutions as well as solids (Robinson, 1996).

2.4.2 INDUCTIVELY COUPLED PLASMA OPTICAL EMISSION SPECTROMETRY

Inductively coupled plasma optical emission spectrometry (ICP-OES), also referred to as inductively coupled plasma atomic emission spectroscopy (ICP-AES), is currently a method used by laboratories to determine concentrations of trace elements in biological samples (Iyengar, 1989).

In 1964 the first report on the use of an inductively coupled plasma optical emission spectrometer for elemental analysis was published by Stanley Greenfield of Birmingham, England (Boss & Fredeen, 2004; Wang, 2004). Velmer Fassel is generally credited with refinements in the ICP analysis and he and his colleagues at Iowa State University, made ICP more practical to analyse nebulised solutions via OES (Wang, 2004).

ICP-OES detects trace elements by producing excited atoms and ions. These excited atoms and ions emit electromagnetic radiation that is detected at wavelengths that are specific to a particular element (Bezerra, Bruns & Ferreira, 2006). In order to produce these excited atoms and ions a plasma flame at a temperature ranging between 6000 - 10 000 K is used (Boss & Fredeen, 2004). At these high temperatures the sample first dissociates into atoms followed by collisions of these atoms. These collisions cause collisional excitation as well as ionisation of atoms (Thomas, 2013). After excitation, atoms and ions decay to lower states through emission energy transitions. Measuring the light emitted at specific wavelengths during this decay of atoms and ions, the concentrations of trace elements can be determined (Wang, 2004).

Argon gas is mostly used to create the plasma flame (Thomas, 2013). Three concentric tubes constructed from quartz form a torch through which the Argon gas is then directed (Boss & Fredeen, 2004). The top end of the torch is surrounded by a copper coil. This copper coil is called the load coil. The load coil is in turn connected to a radio frequency (RF) generator (Boss & Fredeen, 2004). An alternating current is produced within the coil by applying between 700 – 1500 Watts of power to the load coil. The rate at which the current oscillates within the coil corresponds directly to the frequency of the RF generator which in most ICP units is either 27 or 40 megahertz (MHz) (Wang, 2004). This oscillating current induces electric and magnetic fields at the top of the torch.

When argon gas moves through the torch a spark (very brief electric discharge) to the gas is produced by a Tesla unit. The electric discharge produced by the Tesla unit causes some of the argon atoms to lose electrons (Thomas, 2013). These stripped electrons are trapped within the magnetic field in the area at the top of the plasma torch. Acceleration of these trapped electrons are induced within the magnetic field. Energy added to the electrons in this manner is called inductive coupling (Boss & Fredeen, 2004). This sets off a chain reaction in which these high-energy electrons collide with more argon atoms. This causes the argon gas to be transformed into plasma. This plasma consists of argon atoms, electrons and argon ions (Thomas, 2013). The formation of this plasma is called an inductively coupled plasma (ICP) discharge (Wolf, 2013).

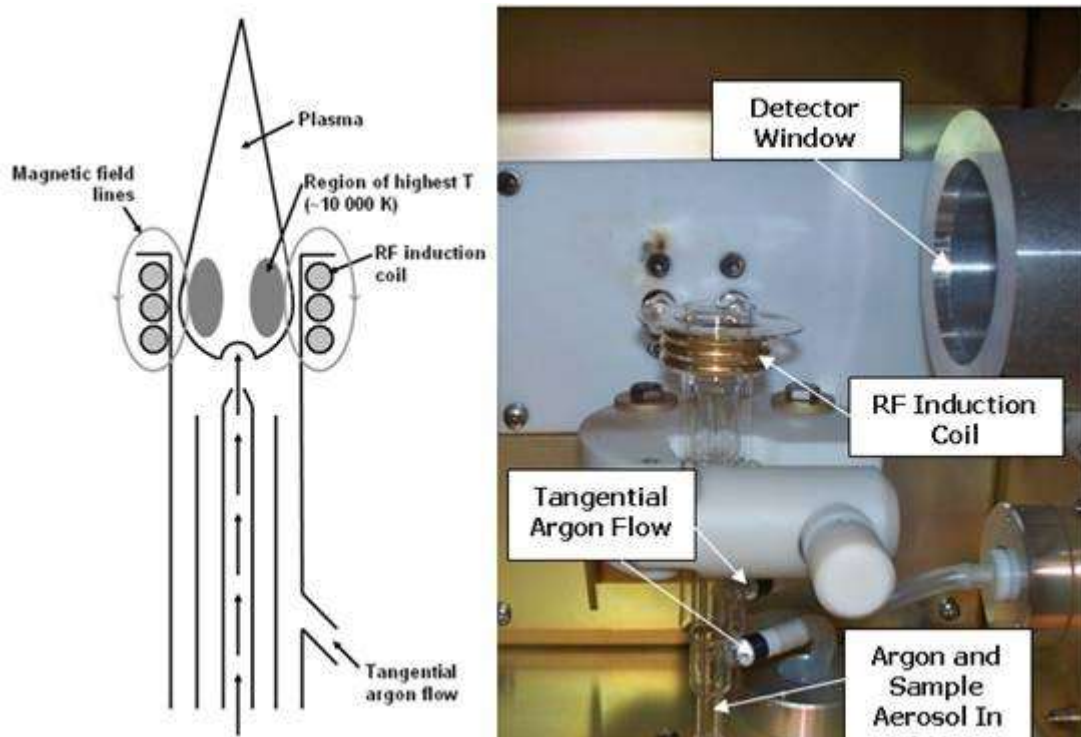


Figure 2.4.2 Different components of the plasma torch in ICP (Concordia College, 2016).

The sample to be analysed is delivered by a peristaltic pump into a nebuliser. The sample is changed into mist within the nebuliser from where the mist is delivered straight into the plasma flame (Thomas, 2013). This is where the sample collides with the electrons and ions within the plasma and the sample itself transformed into ions (Wolf, 2013). The radiation emitted from the sample are then focussed by transfer lenses on a diffraction grating. The diffraction grating forms part of the optical spectrometer and is by far the most common method used (Boss & Fredeen, 2004). From this diffraction grating the monochromatic radiation emitted from the sample are separated into different wavelengths within the optical spectrometer. These different wavelengths are called spectral orders (Wang, 2004).

Multi-elemental analysis of a sample within the spectrometer happens in one of two ways. If the spectrometer consists of multiple exit slits and detectors in which each detector and slit is specific for different wavelengths, the spectrometer is called a polychromatic spectrometer (Boss & Fredeen, 2004). If the spectrometer only has one exit slit and detector that rapidly moves from one wavelength to the next, the spectrometer is called a monochromatic spectrometer (Boss & Fredeen, 2004). Polychromatic spectrometers have a higher sample throughput rate than a monochromatic spectrometer (Wang, 2004). This is because polychromatic spectrometers can analyse a certain number of wavelengths at once whereas monochromatic spectrometers have to move between wavelengths in order to be detected and analysed (Wang, 2004).

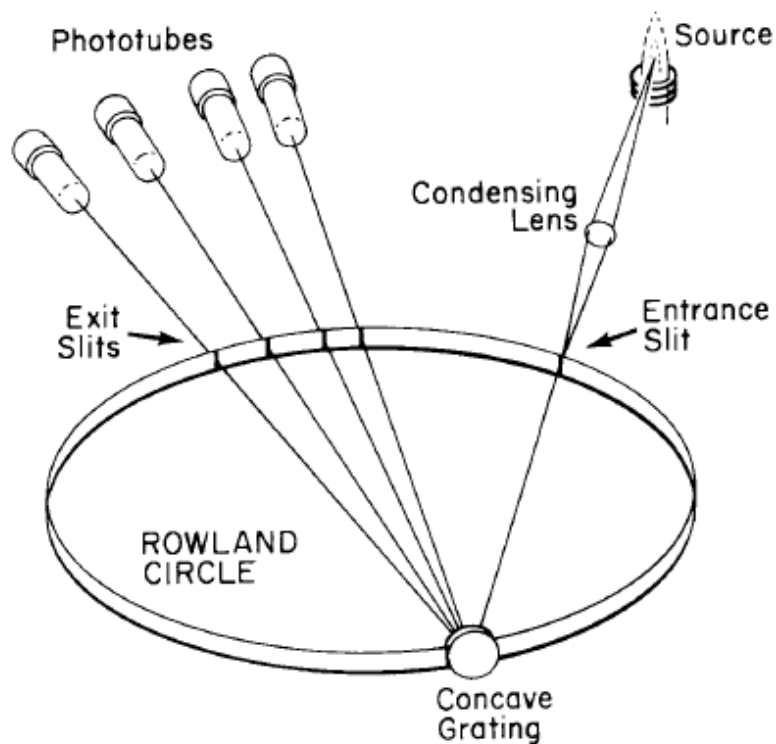


Figure 2.4.3 Example of a circle polychromator (Boss & Fredeen, 2004).

Monochromatic spectrometers have an advantage over polychromatic spectrometers in that they have the ability to access any wavelength at any time within the spectrometer's range (Wang, 2004). Monochromatic spectrometers are therefore superior in their spectral flexibility when compared to polychromatic spectrometers.

After the different wavelengths have been separated and detected by the spectrometer, the wavelengths are converted into electronic signals. These electronic signals are then converted into the different concentrations of trace elements present within the original sample by converting the electronic signal into digital code.

The following diagram illustrates the basic layout of a typical ICP-OES spectrometer.

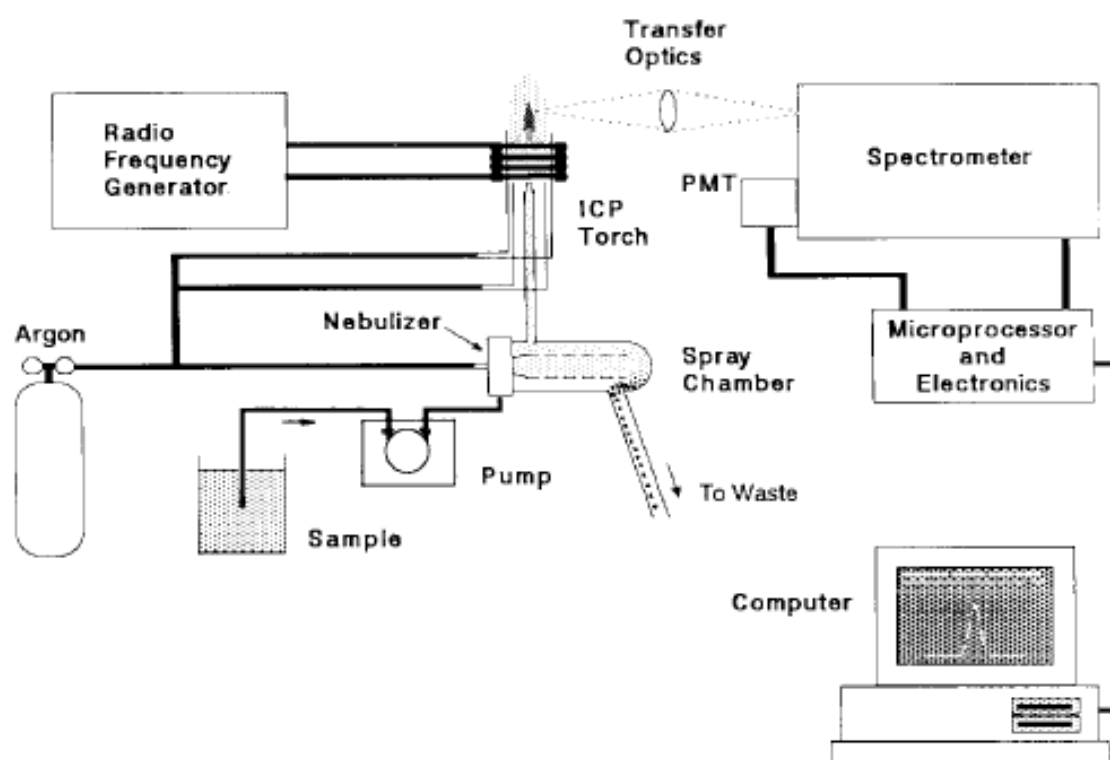


Figure 2.4.4 Layout of a typical ICP-OES instrument (Boss & Fredeen, 2004).

2.4.3 INDUCTIVELY COUPLED PLASMA MASS SPECTROMETRY

Inductively coupled plasma mass spectrometry (ICP-MS) is currently the most sensitive method of detecting trace elements in the medical, forensic and veterinary fields. ICP-MS is capable of detecting trace elements at concentrations as low as one part per trillion (Wolf, 2013).

ICP-MS was first commercialised in 1983 (Thomas, 2004). The two main components of an ICP-MS are the inductively coupled plasma and the mass

spectrometer. As in ICP-OES a plasma torch is also incorporated in the design of an ICP-MS instrument. In ICP-MS the inductively coupled plasma principle is the same as for ICP-OES in that a high temperature plasma discharge is formed, but this is where the similarity between ICP-OES and ICP-MS ends. It is also important that the components and mechanisms of the mass spectrometer are discussed because this is the component of an ICP-MS instrument that is distinctly different from an ICP-OES instrument (Thomas, 2013).

The following diagram illustrates the basic instrumental components of an ICP-MS instrument.

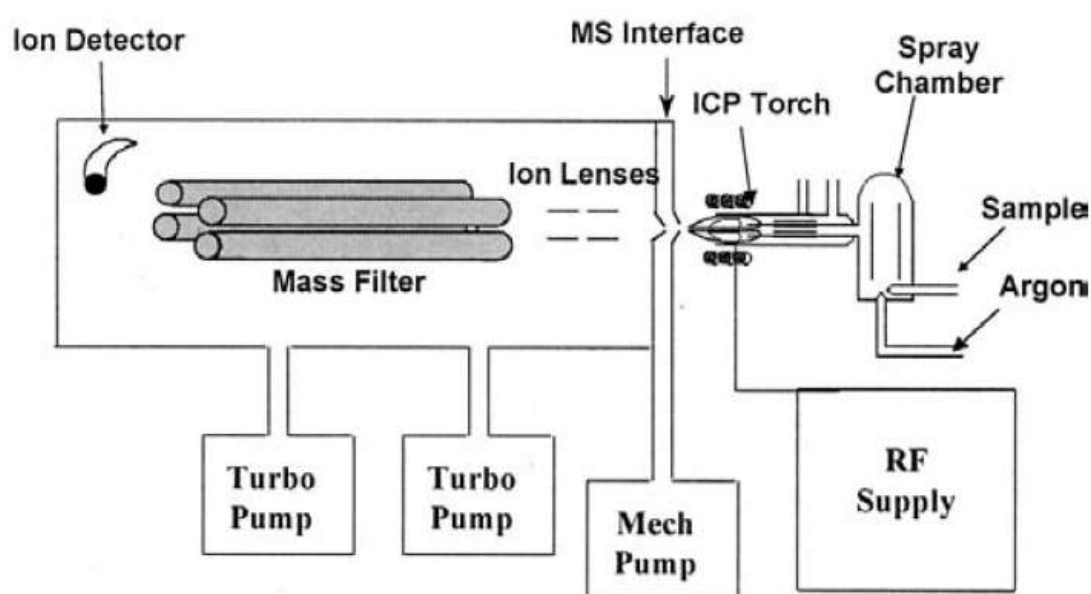


Figure 2.4.5 Components of an ICP-MS instrument (Thomas, 2004)

In ICP-MS the plasma torch is positioned in a horizontal manner as illustrated in Figure 2.4.5. Instead of photons being generated as in ICP-OES, positively charged ions are formed when a nebulised sample passes through the plasma flame in ICP-MS (Thomas, 2004). In ICP-MS, photons are inhibited from reaching the detector. This inhibition of photons reaching the detector results in a decreased signal noise (Thomas, 2013). The low parts per trillion (ppt) detection sensitivity in ICP-MS can be largely contributed to the fact that photons are prevented from reaching the detector (Thomas, 2013). The detection sensitivity

in ICP-MS can also be contributed to the production and detection of large quantities of positively charged ions (Thomas, 2004).

After generation of positively charged ions by the plasma discharge, these ions reach the interface region of the mass spectrometer. The interface consists of two cones. These cones are metallic and are usually constructed using nickel. The two cones are known as the sampler cone and the skimmer cone (Thomas, 2013). The interface region is maintained at a vacuum of 1-2 Torr. The vacuum maintained at the interface region is created by a mechanical pump (Wolf, 2013) as illustrated in Figure 2.4.5. Each cone has a small hole of about 1 mm in the centre through which ions pass onto ion lenses which directs the ions into the mass spectrometer. The sampler and skimmer cones sample the centre portion of the ion beam created at the plasma torch. Photons are prevented to enter the mass spectrometer by a shadow stop (Thomas, 2013). As mentioned earlier, ions pass through each small orifice in each cone after which the ions are directed via ion optic lenses to a mass separation device in the mass spectrometer (Thomas, 2004).

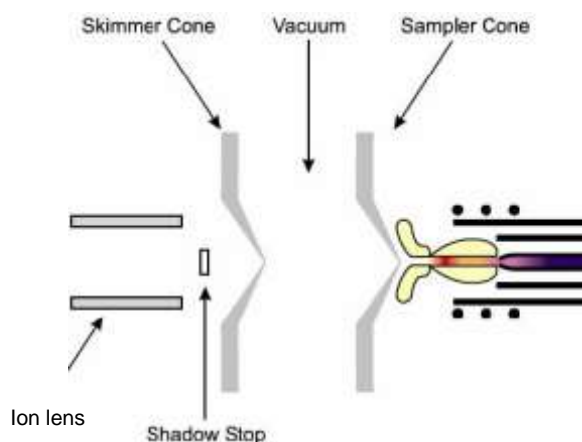


Figure 2.4.6 Interface region of ICP-MS instrument (Wolf, 2013).

The mass separation device is the heart of the mass spectrometer. It is kept at a vacuum of 10^{-6} Torr by a turbomolecular pump (Thomas, 2013). Different types of mass separation devices exist, but basically serves the same purpose. The purpose of the mass separation device is to filter out all non-analyte and matrix-interfering ions. The mass separation device only allows specific analyte ions to reach the detector (Wolf, 2013). The ion detector then converts the analyte ions

into an electrical signal (Thomas, 2004). The electrical signal is then converted into digital code. This digital code is then interpreted as the analyte concentration data. ICP-MS can analyse samples in ppm, ppb and ppt. ICP-MS is a more expensive technique than ICP-OES, but about four times more sensitive than ICP-OES in the detection of trace elements. Interfering ions are removed by adding a collision gas (He) or a reactive gas (H₂) into the plasma. A mixture of collisional and reactive gas may also be added. These gases are injected into the plasma as it flows through the skimmer and/or the sampler cone (Thomas, 2004).

2.5 X-RAY FLUORESCENCE SPECTROMETRY

The discovery of X-rays is credited to Wilhelm Conrad Röntgen, a German physicist who was awarded the first Nobel Prize for Physics in 1901 in recognition of his discovery of X-rays (Thrall, 2002). In 1895, Röntgen discovered that by applying a high voltage in a vacuum tube, electrons are accelerated. When these accelerated electrons strike a metal or glass surface inside the tube it would cause fluorescent minerals a distance away from the tube to glow. This would in turn cause photographic film to become exposed (Giancoli, 1998). This led Röntgen to the conclusion that a new type of radiation is responsible for these effects. Röntgen named this new type of radiation X-rays where X resembles the algebraic symbol “x” which means an unknown quantity (Giancoli, 1998).

The construction of the early X-ray spectrometer is contributed to the work of H.G.J. Mosley. Mosley demonstrated in 1913 the relationship between the atomic number (Z) and the wavelength for every spectral series of emission lines specific for an element in the periodic table (Jenkins, 1999).

The first modern commercial X-ray fluorescence (XRF) spectrometer were built in 1948 by Friedmann and Birks (Jenkins, 1999). Their device consisted of a diffractometer and a detection device. The detection device consisted of a Geiger counter.

Up until the 1960's all commercial XRF spectrometers used simple air path conditions. During the 1960's vacuum or helium paths were incorporated into XRF spectrometer designs (Jenkins, 1999). This allowed for the detection of lighter elements. Lithium fluoride crystals were also introduced during the 1960's for diffraction purposes. During this time target X-ray tubes were constructed from

chromium and rhodium to allow for the excitation of longer wavelengths (Jenkins, 1999).

Lithium drifted silicon detectors (Si(Li)) was created in 1970. These detectors provided very high resolution, as well as providing a higher level of X-ray photon separation (Jenkins, 1999). Silicon drift detectors are still in use today in the construction of XRF spectrometers.

When using XRF spectrometry a sample is irradiated by X-rays (photons). In most cases the source of the radiation is the X-ray tube.

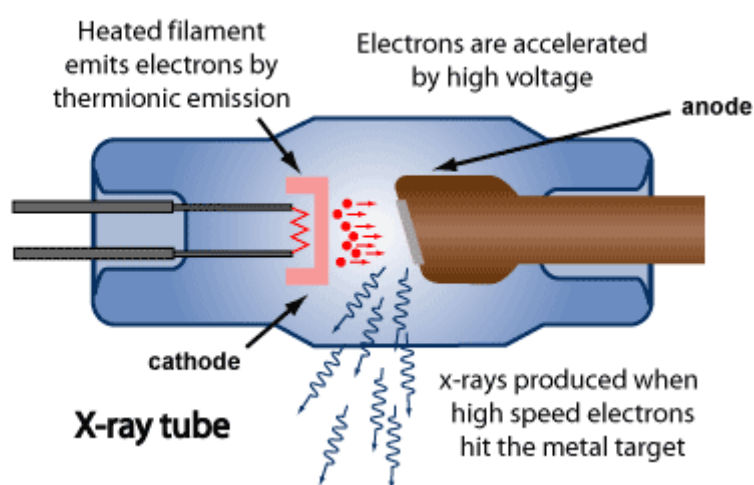


Figure 2.5.1 Components of an X-ray tube

(www.arpana.gov.au/radiationprotection/basics/x-rays.cfm, 05/06/2016).

A radioactive material or synchrotron can also be utilised as sources of radiation in XRF spectrometry (Beckhoff *et al*, 2006). A synchrotron is a type of particle accelerator. When matter comes into contact with X-rays three types of interactions occur. These interactions are fluorescence, Compton scatter and Rayleigh scatter (Thrall, 2002). The inelastic scattering of a photon by a charged particle is called Compton scattering. An example of a charged particle is an electron (Thrall, 2002). Scattering of photons by molecules in the air is called Rayleigh scattering (Thrall, 2002). The fraction of the X-ray radiation that are being absorbed by the sample produces fluorescent radiation (Thrall, 2002).

An atom consists of a nucleus surrounded by electrons. The nucleus consists of positively charged protons and non-charged neutrons (Giancoli, 1998). Grouped

in shells or orbitals surrounding the nucleus are the negatively charged electrons (Giancoli, 1998). The orbitals surrounding the nucleus are named according to their distance from the nucleus. The innermost orbital is called the K-shell followed by the L-shell, M-shell, N-shell etc. (Giancoli, 1998). When an atom is irradiated by an X-ray with sufficient energy, electrons can be expelled from their specific orbitals (Figure 2.5.2). If an electron is being expelled from the K-shell by an X-ray, a vacancy is being created in the K-shell (Thrall, 2002). This causes a disruption in the original configuration of the atom. To compensate for this disruption an electron from an outer orbital, such as the L-shell, fills the vacancy within the K-shell. Electrons within the L-shell has a higher energy potential than electrons within the K-shell (Giancoli, 1998). When a L-shell electron fills the vacancy within the K-shell, excess energy is being released in the form of photons. This is called fluorescent radiation (Beckhoff *et al*, 2006).

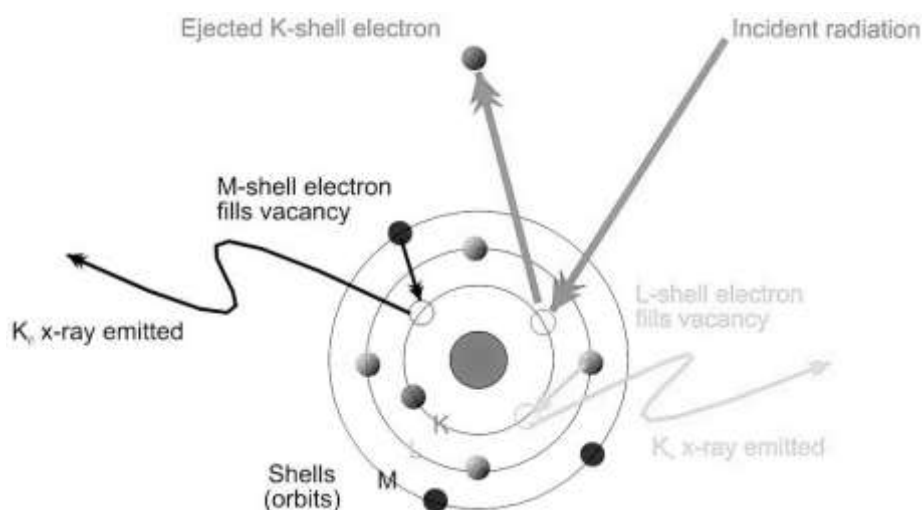


Figure 2.5.2 Incident radiation causing X-ray fluorescence (Bruker, 2016).

The atoms of each element have its own specific energy levels unique to the element involved. This makes it possible to differentiate between elements depending on the type of fluorescent radiation being emitted (Beckhoff *et al*, 2006). This is the principle on which XRF spectrometry works.

Two types of XRF spectrometers are distinguished depending on their mechanism of detecting the fluorescent radiation. The two types of spectrometers are called wavelength dispersive XRF and energy dispersive XRF. Wavelength

dispersive XRF spectrometers are typically found as large instruments fitted in a laboratory whereas energy dispersive XRF spectrometers are included in handheld XRF models. Bench-top XRF instruments are designed to either be wavelength dispersive or energy dispersive.



Figure 2.5.3 Energy dispersive benchtop XRF spectrometer (Oxford instruments, 2016).

In wavelength dispersive XRF a sample emits X-rays after being irradiated by an X-ray source. These X-rays that are emitted by the sample have characteristic wavelengths unique to the elements present within the sample (Helsen & Kuczumow, 2002). In order to divide the incoming X-rays emitted from the sample before it reaches the detector, a diffraction mechanism is placed between the incoming X-rays and the detector within the spectrometer. By manipulating the angle of the diffractor between the incoming X-rays and the detector, certain wavelengths can be targeted and the wavelengths reaching the detector can be controlled in this manner (Helsen & Kuczumow, 2002). This makes it possible to sequentially measure elements of interest.

In energy dispersive XRF the sample also emits X-rays after being irradiated by an X-ray source. Energy dispersive XRF analysers are designed in two ways. In the first design the X-ray beam is aimed directly at the sample. This leads to direct excitation of the sample being analysed (Ellis, 2002). In the second design the analyser incorporates a secondary target. The X-ray source is directed at this secondary target which then leads to excitation of the secondary target. The fluorescence emitted by the secondary target acts as a source of excitation to excite the sample being analysed (Ellis, 2002). In both designs a detector measures the incoming fluorescence and assigns an energy value to each fluorescent pulse reaching the detector.

Wavelength dispersive XRF spectrometers have a higher resolution (Helsen & Kuczumow, 2002) than energy dispersive XRF models and are superior in terms of high precision analysis of samples. The advantages of energy dispersive XRF models are that they are smaller, simpler in design and have fewer engineered parts.

In a study conducted in 2012 involving a bench-top energy dispersive XRF model, goat tibiae were used to detect concentrations of lead in the bones and compared the XRF results to ICP-MS analysis of the same bone samples. Concentrations measured by the bench-top XRF analyser proved to be very reliable when compared to concentrations obtained from the ICP-MS analysis (Bellis, Todd & Parsons, 2012).

2.6 HANDHELD X-RAY FLUORESCENCE SPECTROMETRY

Handheld XRF spectrometers are being used in a wide variety of fields ranging from geology, mining, archaeology, forensics, art and environmental science. The handheld XRF analysers are energy dispersive spectrometers and are smaller, simpler in design and cheaper than the large laboratory wavelength dispersive XRF spectrometers (Beckhoff *et al*, 2006).

The basic components of a handheld X-ray fluorescence spectrometer include an X-ray source, a detector, a digital signal processor, a central processing unit

(CPU), a screen from which analysed data can be interpreted, a universal serial bus (USB) port to which a laptop can be connected and an internal storage unit (Thermo-Scientific, 2016). All of these components are assembled in a rugged casing much resembling a pistol. The operator holds the handheld XRF spectrometer in one hand and point the end emitting the high energy X-rays towards the sample being analysed. Scatter radiation are very limited due to the small collimated area at the end from which X-rays are emitted. This safeguards the operator of the handheld XRF spectrometer to any risk of exposure to radiation. All elements present in the sample will appear on the spectrometer's screen within a minute or two. Concentrations of elements are displayed in ppm.

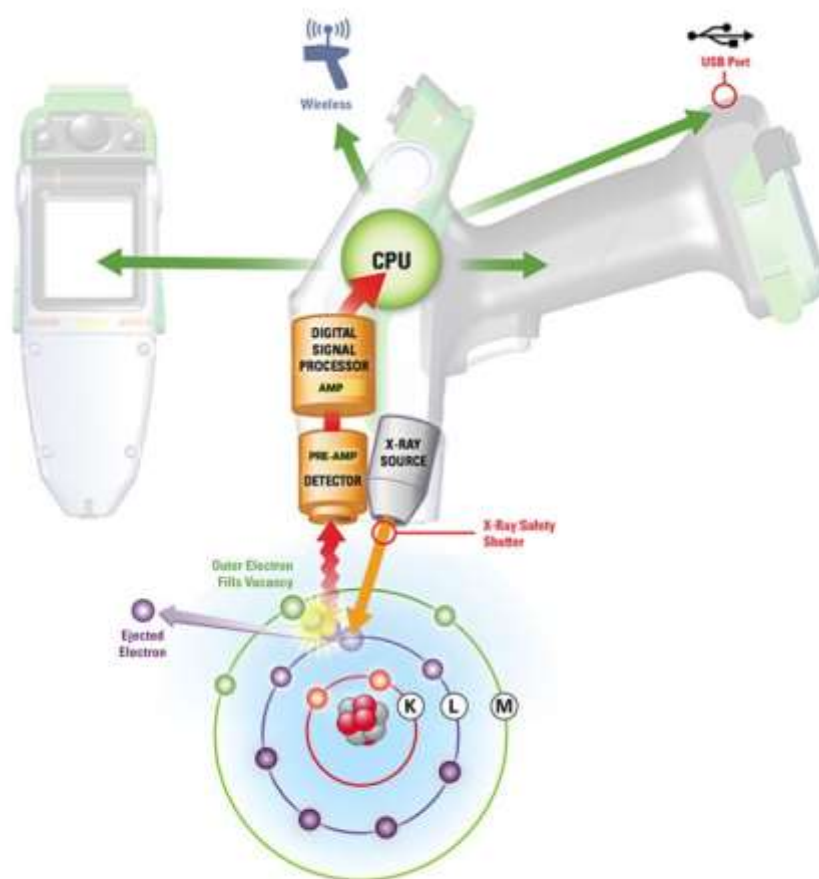


Figure 2.6.1 Image of a handheld X-ray fluorescence spectrometer (Thermo-Scientific, 2016).

Literature reporting on the use of handheld XRF spectrometers to study human or animal tissue is limited. In an anthropological study conducted in 2013, the investigators used a handheld XRF spectrometer to distinguish human osseous and dental tissue from non-human material of similar elemental composition (Zimmerman, 2013). In a more recent forensic anthropological study published in 2016, a handheld XRF spectrometer was used to determine elemental profiles in bones from four mammal species. The handheld XRF spectrometer was used to analyse human, elephant, dog and dolphin bones in order to determine the elemental profiles of each species (Nganvongpanit *et al*, 2016).

No previous studies or research that has been conducted using a handheld XRF spectrometer to determine concentrations of important trace elements in ovine livers or any other species of veterinary importance were found. A gap therefore exists in the current knowledge concerning the use of handheld XRF spectrometers to determine important trace elements in veterinary diagnostics.

2.7 AIM

The aim of the research project is to ascertain if the handheld X-ray fluorescence spectrometer will provide reliable concentrations of certain essential trace elements in the livers of sheep.

2.8 OBJECTIVES

The objectives of this study were:

- to collect data sets from trace element concentrations obtained from ovine liver samples measured by handheld X-ray fluorescence.
- to compare these data sets to trace element concentrations obtained from ovine liver samples determined by a reference laboratory (control).

CHAPTER 3

MATERIALS AND METHODS

3.1 EXPERIMENTAL DESIGN

3.1.1 MODEL SYSTEM

This is a quantitative experimental research study involving important trace element concentrations in ovine liver as determined by handheld X-ray fluorescence spectrometry. Due to a lack of data using handheld X-ray fluorescence spectrometry to determine concentrations of important trace elements in ovine livers, this research project can also be considered a pilot study with the aim of gathering information to inform future studies.

3.1.2 LIVER SAMPLES

Livers, weighing approximately 900 g, of 10-month old South African Mutton Merino lambs were collected from Cavalier abattoir situated on the farm “Oog van Boekenhoutskloof” near Cullinan, Gauteng Province. The livers were vacuum packed and stored at -20°C until further processing. Ventral (left) lobes from each liver were subjected to analysis of certain trace minerals during this study. Samples were taken randomly from each left liver lobe. There seems to be a trend toward increased concentrations of important trace minerals (especially copper) within the ventral (left) lobe when compared to concentrations of trace minerals within the dorsal (right) lobe in the livers of lambs (Hogan *et al.*, 1971). In mature sheep, the distribution of trace minerals become more homogeneously dispersed throughout the liver (Hogan *et al.*, 1971).

3.2 EXPERIMENTAL PROCEDURES

3.2.1 PREPARATION OF LIVER SAMPLES FOR ANALYSIS

Prepared liver samples were analysed by handheld XRF spectrometry and ICP-MS.

3.2.1.1 Preparation of liver samples for XRF spectrometry

Ovine livers (n=30) were placed in a refrigerator at 4°C for 4 h until semi-thawed. Using a scalpel, the left lobes were removed. Scalpel blades were changed between liver samples to avoid cross contamination. After the left lobes were separated, 3 portions, weighing 20, 70, and 150 g respectively, were cut from each lobe. The 20 g samples of liver were stored at -20°C until XRF spectrometry was performed. The liver samples were marked WB 1 - WB 30 (WB = wet blended). The 70 g liver samples were subjected to oven drying and marked OD 1 - OD 30 (OD = oven dried). The 150 g samples were allocated to be dry ashed and marked DA 1 - DA 30 (DA = dry ashed). The 70 g and 150 g samples were also stored at -20°C until ready for further preparation.

Oven drying of liver samples for XRF analysis

A Labex oven (Labcon) was used for the drying procedure. The oven drying procedure was performed at the Pharmacology and Toxicology Laboratory, Department of Paraclinical Sciences, Faculty of Veterinary Science, University of Pretoria. The oven was set at 50°C and the temperature within the oven was monitored. The 70 g liver samples were cut into slivers (1 – 2 mm) using a scalpel. Scalpel blades were changed between samples. The slivers were then placed in shallow Pyrex glass containers (8 cm in diameter) and dried until the weight remained constant. The weight of each Pyrex container was also recorded to ensure the containers all weighed the same.

The drying oven could only accommodate 15 Pyrex glass containers at a time. Liver samples marked OD 1 - OD 15 were first prepared for drying (see Figure 3.2.1).



Figure 3.2.1 Marked liver samples in drying oven.

Liver samples were weighed at 24 h after the samples were placed in the oven and again at 48 and 54 h. Constant mass was achieved at 54 h after the wet liver samples were placed in the drying oven. After liver samples OD 1 - OD 15 were oven dried the same drying procedures were repeated for liver samples OD 16 - OD 30.

The samples were then pulverised to form a fine homogenous powder. This was achieved using a porcelain mortar and pestle (see Figure 3.2.2). Each dried liver sample were broken up into smaller pieces by hand and placed within the mortar and pestle. By grinding the sample in the mortar with the pestle a fine homogenous powder was produced after about 30 min. The mortar and pestle were cleaned between samples using 70% ethanol to avoid cross-contamination. The homogenous powder of each sample was placed in a plastic bag and

vacuum sealed. Each bag was marked with the sample number (for example OD 1, OD 2, OD 3 etc.).



Figure 3.2.2 Mortar and pestle with oven dried sample.



Figure 3.2.3 Vacuum sealed homogenous powder (left) with vacuum sealer in background. Ethanol spray and mortar and pestle to the right of photo.

The vacuum sealed oven dried liver samples were stored at room temperature until the XRF analysis was performed on each sample.

Dry ashing of liver samples for XRF analysis

Dry ashing of liver samples was done at Nutrilab, Faculty of Natural and Agricultural Sciences, University of Pretoria. The vacuum sealed liver samples weighing 150 g each and marked DA 1 - DA 30 were dry ashed. Each liver sample was cut into slivers using a scalpel. The slivers were placed into 15 cm x 10 cm aluminium foil containers. Scalpel blades were changed between samples. The aluminium foil containers were weighed to verify that all the containers are of the same weight. Two drying ovens (Merck Laboratories) were set at 55°C and the temperature within the ovens monitored. Liver samples DA 1- DA 30 were placed in the two drying ovens and constant weight was achieved after 48 h. The dried liver samples were broken into smaller pieces and ground to a powder using a mortar and pestle as described above.



Figure 3.2.4 Labcon muffle furnaces at Nutrilab laboratories.

Four small porcelain crucibles were used per liver sample. Using the Mettler scale 5 g of powdered liver sample were placed in each crucible. Great care was taken because if more than 5 g was used per crucible the sample would “explode” in the furnace causing cross contamination between samples. For each liver sample a total of 20 g were used (4 crucibles containing 5 g each). Each crucible was

stamped with a number and for each liver sample the numbers of the 4 crucibles used for that specific sample was noted in an A5 manuscript book. The livers were ashed in 3 batches over a period of 6 days in two Labcon muffle furnaces (ash ovens).

The muffle furnaces were heated to a temperature of 250°C before the crucibles were placed within the ovens. The samples were then ashed for 2 h at 250°C. After 2 h, the temperature of the furnaces was increased to 550°C. The samples were left at this temperature for 5 h where after the muffle furnaces were switched off and left overnight to cool off. The ashed samples were collected the following morning. Approximately 2 g of ash were produced from each sample. The ash of each sample was placed within a plastic bag and vacuum sealed. Using a black permanent marker, each sealed bag was marked with the sample it contained (for example DA 1, DA 2 etc). The sealed ash samples were stored at room temperature until ready to be analysed by XRF spectrometry.



Figure 3.2.5 Crucibles with finished ash samples within muffle furnace.

3.2.1.2 Preparation of liver samples for ICP-MS analysis

Fifty gram segments were cut from the left lobes of the 30 semi-thawed livers. Each of these liver samples were vacuum sealed and the bag marked with a black permanent marker. The samples were individually marked as L1 - L 30 (L= laboratory). The samples were stored at -20°C until delivery to NviroTek Laboratories situated in Ifafi, Hartbeespoort, North West Province.

The 50 g liver samples were further prepared for ICP-MS analysis at NviroTek. Three small (5 mm) cubes were cut from each 50 g sample. Excess liver was stored at -20°C. The three small cubes per liver sample were taken as one sample, one control and one for moisture determination.

3.2.2 ANALYSIS OF PREPARED LIVER SAMPLES

3.2.2.1 Handheld X-ray fluorescence spectrometry

All XRF spectrometer analyses were performed at the Pharmacology and Toxicology Laboratory.

X-ray fluorescence instrumentation

An Olympus Delta Premium 6000 handheld XRF spectrometer were supplied by Innov-X-Africa, Bedfordview, Gauteng Province. The Olympus Delta Premium 6000 XRF spectrometer (serial number 512000) consists of a Rh anode tube and a large area silicon drift detector (SDD). Also included were a waterproof Pelican carry case, 2 Li-ion batteries, docking station/battery charger, mini USB cable, a 316-calibration check stainless steel reference coin, Advanced Delta PC software and an Asus laptop with Windows 10 Professional, a portable workstation, polyethylene sample cups and a roll of Mylar sample film.



Figure 3.2.6 Olympus Delta Premium 6000 XRF spectrometer in carry case.

The Olympus Delta Premium XRF unit was set to the Geo-chemistry (soil) mode. In this mode, the XRF unit operates a dual beam fundamental parameter algorithm optimized for achieving lowest limit of detection (LOD) for exploration samples. The dual beam consists of a 40 KV and 15 KV beam. The 40 KV beam was set to operate at two different configurations. This means that the 40 KV beam acted as if it was two separate beams. Elements detected by the 40 KV beam in its 1st configuration (beam 1) = U, Sr, Y, Zr, Mo, Ag, Cd, Sn, Sb, Ti, V, Cr, Mn, Fe, Co, Ni, Cu, Zn, W, Hg, As, Se, Pb, Th and Rb. Elements detected by the 40 KV beam in its 2nd configuration (beam 2) = Fe, Co, Ni, Cu, Zn, W, Hg, As, Se, Pb, Bi, Rb, Ti, V, Cr, Mn, U, Sr, Y, Zr, Th, Mo, Ag, Cd, Sn and Sb. Elements detected by the 15 KV beam (beam 3) = P, S, Cl, K, Ca, Ti, V, Cr, Mn and Fe. Using the Advanced Delta PC software, the unit was set to only detect concentrations of Cu, Fe, Mn, Mo, Se and Zn in the samples analysed.

The front area of the XRF unit from where X-rays are emitted, are covered with a Prolene window film. This window film protects the XRF from dust and other

environmental contaminants. The X-ray beam emitted from the front end of the XRF unit has a diameter of approximately 10 mm.

The handheld XRF unit was attached in an inverted position to the workstation (see Figure 3.2.7). The sample to be analysed was placed in the chamber of the workstation and the lid closed. During analysis, a blinking light was displayed from the workstation's lid. The workstation was connected to a 240 V electrical socket thus supplying power to the XRF unit and the components of the workstation. The Asus laptop was connected via an USB port to the Olympus workstation (see Figure 3.2.8). This allows for data in ppm obtained from analysing samples to be imported to the Advanced Delta PC software on the laptop. From the Delta PC software, data could be exported to Microsoft Excel and saved as an Excel spreadsheet.



Figure 3.2.7 Olympus Delta XRF unit attached in an inverted position to the workstation with sample chamber.

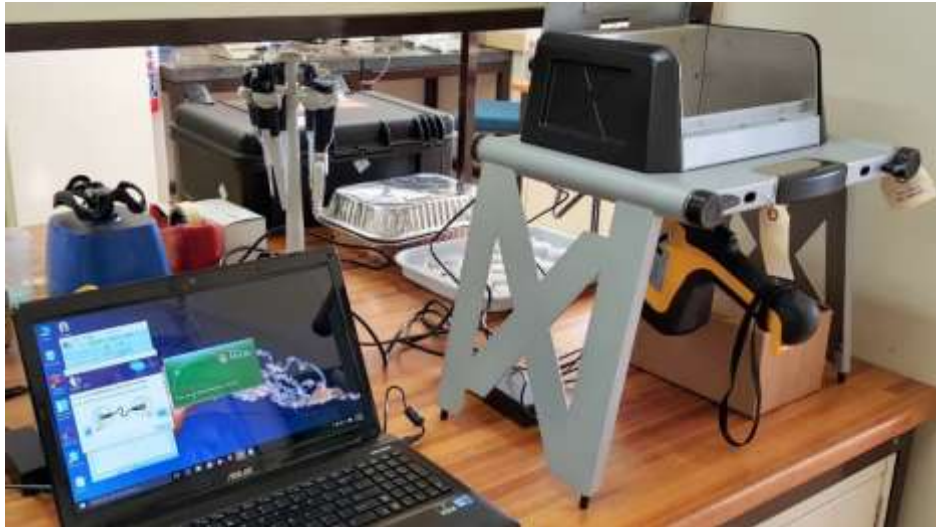


Figure 3.2.8 Laptop connected to workstation via USB cable.

SPEX® SamplePrep closed x-cell polyethylene sample cups (n=90) were used (code no SPEX-3527). Each sample cup had a diameter of 40 mm and an aperture diameter of 31.5 mm. The maximum capacity of each sample cup was 13 ml.

The film used to cover the sample cups was a roll of 0.25 mm thick x 7 cm wide Mylar (code no SPEX-3517) (Figure 3.2.9). Mylar film is cost effective, has a high tensile strength and is strong and robust for field use.



Figure 3.2.9 Mylar film roll and polyethylene sample cup (left). Stainless steel calibration coin in workstation's test chamber (right).

A calibration check was done each morning before liver samples were analysed. The 316-stainless steel calibration coin was used to perform the calibration checks (see Figure 3.2.9). Calibration check ensures that the XRF spectrometer is reading correctly and within the limits set out during initial calibration.

XRF analysis of wet blended liver samples

The wet blended samples marked WB 1 – WB 30 were analysed by XRF spectrometry. Each sample was subjected to 5 analyses (readings), which amounted to a total of 11.25 min (675 s) per sample. In addition to the initial five readings per sample, four random duplicates of WB 1 – WB 30 were picked by re-arranging the sample cups randomly on a table and blindly picking four samples. The duplicates were marked WBD (wet blended duplicate).

Each 20 g wet liver sample was placed in a 50 ml glass beaker. Using the DIAX 600 homogenizer each sample was blended until a smooth homogenous mass. After a sample was homogenised, the sample was placed in a SPEX® SamplePrep sample cup. Approximately 13 g was used per sample to fill the cup (maximum volume per cup = 13 ml). After filling a cup, a piece of Mylar film was placed over the top of the cup. The Mylar film was secured in place using a polyethylene ring. Each cup was marked with the number allocated to the sample (WB 1 – WB 30), using a black permanent marker. The sample cups were each individually placed in the workstation's test chamber. The sample to be analysed was placed in an inverted position over the opening in the test chamber where the front end of the XRF spectrometer attached to the chamber was located. After closing the test chamber's lid the sample was analysed. A blinking light on the lid of the chamber indicated that the analysis was in progress. After the analysis was completed the blinking light stopped and the chamber opened.



Figure 3.2.10 Placing piece of Mylar film over sample cup (left). Placing polyethylene ring on top of Mylar film and securing film in place by pressing down on polyethylene ring (right).



Figure 3.2.11 Finished sample cups after Mylar film has been secured and sample cups marked (left). Sample cup in inverted position in test chamber of Olympus workstation (right).

After each sample was analysed the data (in ppm) of all five readings were imported to the Delta PC software (see Figure 3.2.12) on the Asus laptop. From the Delta PC software, the data was exported to Excel and saved as an Excel spreadsheet.

XRF analysis of oven dried liver samples

The oven dried samples marked OD 1 – OD 30 were used. Each sample cup was filled with 13 g of the oven dried fine homogenous liver powder. To fill and seal each cup, the steps discussed under XRF analysis of wet blended liver samples were followed.

Duplicates of OD 1 – OD 30 were picked by re-arranging the sample cups randomly on a table and blindly picking four samples. The duplicates were marked ODD (oven dried duplicate). Oven dried samples were each separately placed in the workstation's test chamber and analysed. Five readings were performed on each sample, including the duplicates.

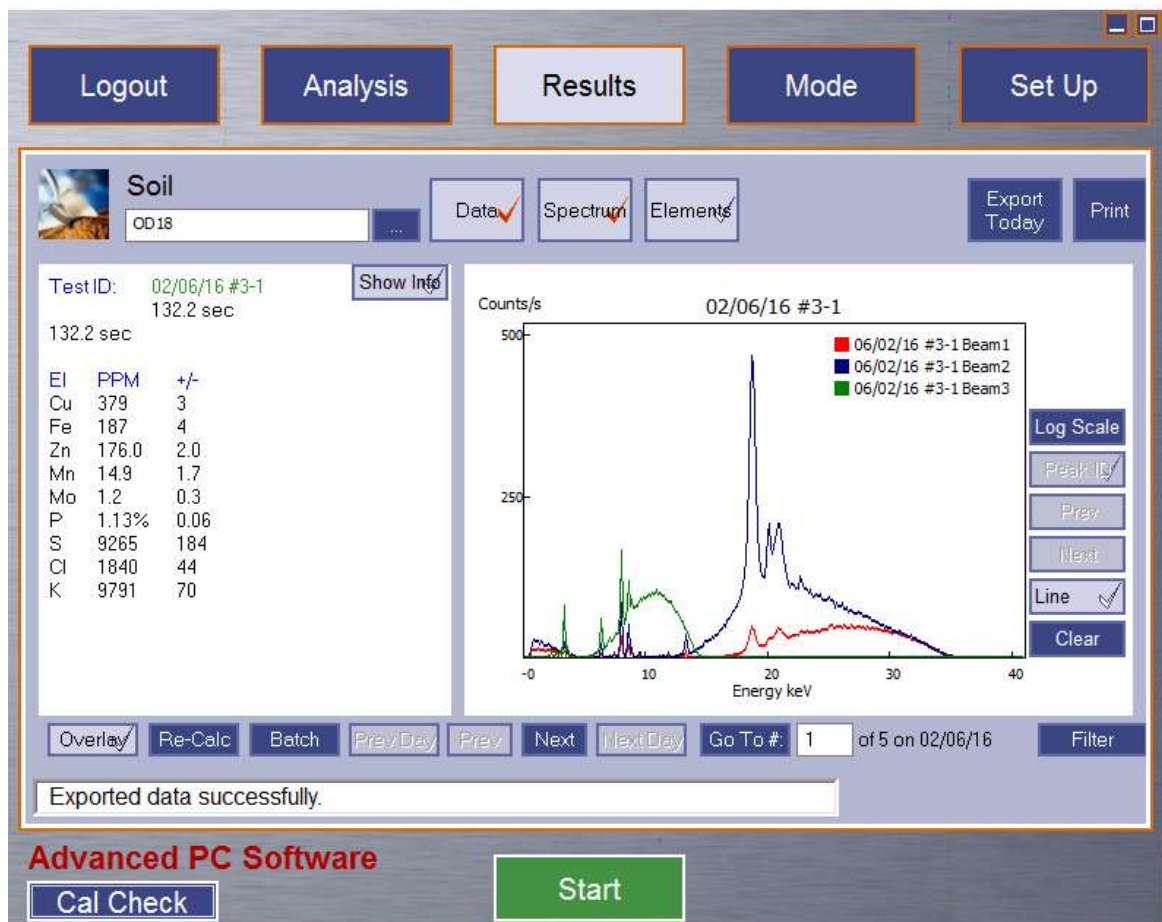


Figure 3.2.12 Advanced Delta PC software with results.

XRF analysis of dry ashed liver samples

Dry ashed samples marked DA 1 – DA 30 were analysed using handheld XRF spectrometry. Duplicates of DA 1 – DA 30 were picked by re-arranging the sample cups randomly on a table and blindly picking four samples. The duplicates were marked DAD (dry ash duplicate).

Due to the small amount of ash ($\pm 2\text{g}$) obtained after ashing of liver samples, a double layer of Mylar film was used to form an “envelope” in which the ashed sample could be firmly secured (Figure 3.2.13). The completed sample cups were separately placed within the test chamber and analysed. Data were exported in the same manner as with the wet blended and oven dried samples.



Figure 3.2.13 Dry ashed sample placed onto bottom piece of Mylar film to prevent sample from falling into sample cup (left). A second piece of Mylar film placed over sample to form an envelope (right).

3.2.2.2 ICP-MS analysis of liver samples performed by reference laboratory

ICP-MS analysis of liver samples was conducted by NviroTek laboratories, situated at Ifafi, Hartbeespoort, North West Province. Liver samples marked L 1 – L 30 were analysed via ICP-MS.

Moisture determination

A porcelain crucible was weighed without the wet liver sample. After weighing the empty crucible, a wet liver sample prepared for moisture determination was placed within the crucible. The crucible with liver inside were then weighed. The wet liver sample was dried in a drying oven at 105°C until constant weight (usually within 24 hours). The weight of the crucible containing the oven dried liver sample was measured. The percentage moisture lost in the liver sample was determined by the laboratory using the following equation:

$$\% \text{ Moisture} = [(\text{mass crucible} + \text{wet liver} - \text{mass crucible} + \text{dry liver}) / \text{mass wet sample}] * 100$$

Digestion of liver samples for ICP-MS analysis

The laboratory weighed ± 1.5 g of wet liver sample in a weighing boat. Using a spatula, the sample was scraped from the weighing boat into a digestion tube. Ten ml concentrated HNO₃ were added to the digestion tube. The sample was pre-digested for 15 min before placing the cap on top and closing the digestion tube. The digestion tubes were placed in accordance to the carousel instructions of the microwave digester. A microfibre sensor were gently placed in digestion tube 1. The liver method was selected on the microwave and the samples digested. After digestion, the tubes were cooled off for 15 min. Wearing gloves and goggles the caps were removed from the digestion tubes. A blank was read for every set of samples placed in the microwave digester.

ICP-MS analysis of digested liver samples

A minimum of 5ml of digested sample was placed in a polypropylene auto-sampler tube. Samples were placed in the auto-sampler tray of the mass spectrometer. The samples were nebulised to form an aerosol. The aerosol

droplets were introduced into an argon plasma torch. The plasma torch dissociates the molecules thus forming singly-charged ions. These ions are directed to the mass spectrometer where the different elements are analysed. The ICP-MS exported the analysed data in $\mu\text{g/L}$ to a computer connected to the ICP-MS unit. The laboratory technologists imported the data into Microsoft Excel and converted the $\mu\text{g/L}$ to mg/L .

CHAPTER 4

RESULTS AND DISCUSSION

Data from the ICP-MS and XRF analyses were captured in Excel spread sheets and statistically analysed, which consisted of three steps:

1. Determine the mean, median and reference ranges (min – max) of all ICP-MS and XRF concentrations of certain trace elements in 30 ovine livers collected at an abattoir in Gauteng and to compare it to diagnostic data as provided by Puls (1994).
2. Determining the precision of tools (ICP-MS and XRF) by element and preparation type.
3. Correlate the results obtained by using Pearson and Bayesian correlation analyses.

4.1 REFERENCE RANGES

Table 4.1.1 Ranges of trace element concentrations (ppm) in ovine livers from Puls (1994).

Element	Wet Weight (WW)		Dry Weight* (DW)	
	Min	Max	Min	Max
Cu	25	100	100	400
Fe	30	300	120	1200
Mn	2	4.4	8	17.6
Mo	0.375	1.5	1.5	6
Se	0.25	1.5	1	6
Zn	30	75	120	300

* Multiplied the wet weight by four to determine the range as dry weight

Table 4.1.2 Concentrations of six trace elements (ppm (DW)) in the ovine liver (n=30) as determined by the reference laboratory (Nvirotek) using ICP-MS analysis.

	Min	Max	Mean	SD	Median
Cu	193	817	428.90	120.88	417.40
Fe	116	586	241.40	98.43	211.90
Mn	5.1	19.5	10.00	2.27	10.80
Mo	2.2	5.3	3.80	0.75	4.10
Se	0.86	2.77	1.60	0.34	1.7
Zn	91	245	129.40	17.01	130.20

Table 4.1.3 Concentrations of six trace elements (ppm) in the ovine liver (n=30) as determined by handheld XRF analysis.

(a) Wet blended concentrations.

Wet blended					
	Min	Max	Mean	SD	
Cu	65.6	230	147	82.2	
Fe	8	116	62	54	
Mn	-	-	-	-	
Mo	-	-	-	-	
Se	-	-	-	-	
Zn	25.7	47.2	36.5	10.8	

(b) Oven dried concentrations.

Oven dry				
	Min	Max	Mean	SD
Cu	221	783	580	204
Fe	93	484	287	102
Mn	4.9	18.5	9.3	2.5
Mo	1	2.1	1.5	0.2
Se	-	-	-	-
Zn	102.7	181	120	21.1

(c) Dry ashed concentrations.

Dry ashed				
	Min	Max	Mean*	SD
Cu	2293	14187	8240	5947
Fe	1218	8651	4935	3717
Mn	60	272	166	106
Mo	7.3	50.5	29	21.6
Se	1.6	2.3	2(7)	0.4
Zn	887	3114	2000	1114

*The number of samples to calculate the mean if less than 30 is indicated in brackets.

For some of the elements, Puls (1994) suggested concentration ranges that increased by an order of magnitude from wet to dry samples. An order of magnitude indicates an increase or decrease in concentration by ten units (two orders of magnitude = 100 units, three orders of magnitude = 1000 units etc.). These elements included Fe and Zn. For some elements only a minimum concentration or maximum concentration increased by an order of magnitude (Cu, Mn). For the other elements, a change from wet to dry samples resulted in ranges that were within the same order of magnitude (Mo, Se). In the wet blended liver samples analysed by XRF spectrometry, the ranges of the three detectable

elements (Cu, Fe, Zn) were generally within the same order of magnitude (no increased or decreased concentrations of more than ten) as compared to reference ranges as suggested by Puls (1994). Mn, Mo and Se were not detectable using the wet blended preparation method for XRF spectrometry (Fig. 4.1.3 a). Using the different preparation methods for XRF spectrometry the concentration ranges of measured elements generally increased by an order of magnitude between wet blended to oven-dried to ashed samples. Some elements also became detectable when analysing oven-dried and/or ashed samples. Mn, Mo and Se were not detectable when using the wet blended preparation method, while only Se was not detectable when the liver samples were oven-dried (Fig. 4.1.3 b). All six elements were detectable in ashed samples, though not in every sample (e.g. Se) (Fig. 4.1.3 c).

Table 4.1.4 Ranges by order of magnitude.

	Puls				ICP-MS		XRF					
	Wet		Dry				Wet		OD*		Dry Ash#	
	Min	Max	Min	Max	Min	Max	Min	Max	Min	Max	Min	Max
Cu	1	2	2	2	2	2	1	2	2	2	3	4
Fe	1	2	2	3	2	2	0	2	1	2	3	3
Mn	0	0	0	1	0	1	-	-	0	1	1	2
Mo	0	0	0	0	0	1	-	-	0	0	0	1
Se	0	0	0	0	0	0	-	-	-	-	0	0
Zn	1	1	2	2	1	2	1	1	2	2	2	3

*Oven dried until a constant weight was achieved

#Dry ashed in a muffled furnace at 550 °C

4.2 PRECISION OF TOOLS (ICP-MS AND XRF) BY ELEMENT AND PREPARATION TYPE

4.2.1 COPPER

Cu was detectable using XRF spectrometry from a low concentration of 65.6 ppm wet weight to a high of 14187 ppm ashed weight, thus spanning at least three orders of magnitude. Precision of the XRF measurement (as indicated by intra-sample coefficient of variation) improved (CV decreased) as the element concentration increased relative to the matrix (i.e. when moving from wet to oven dried to ashed samples). Black dots = sample repeatability according to the median. Grey dots = sample repeatability according to the mean. See Figure 4.2.1.

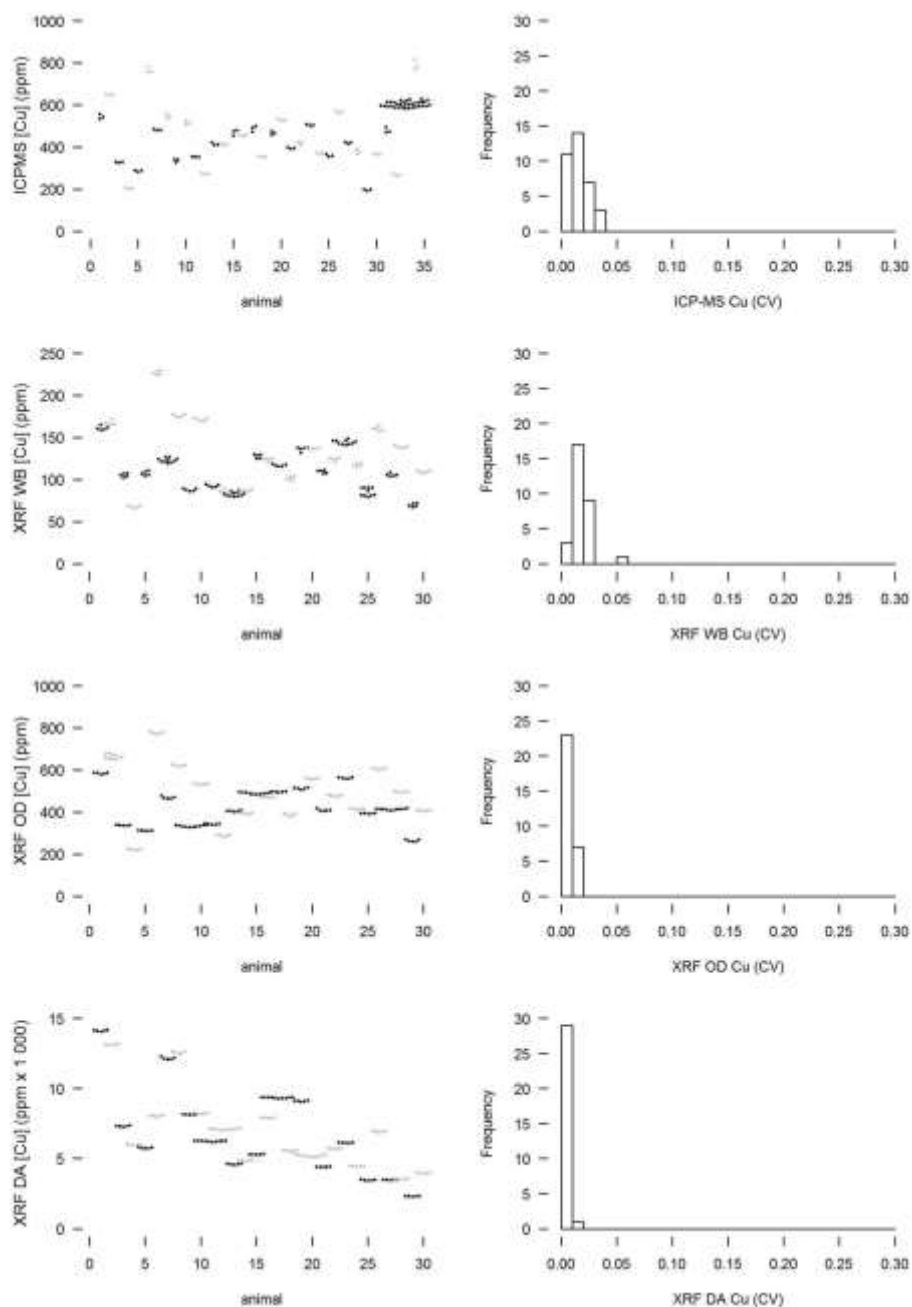


Figure 4.2.1 Cu concentrations as determined by ICP-MS and XRF.

4.2.2 IRON

Fe was detectable using XRF spectrometry from a low concentration of 8 ppm wet weight to a high of 8651 ppm ashed weight, thus spanning at least 4 orders of magnitude. Precision of the XRF measurement (as indicated by intra-sample coefficient of variation) improved (CV decreased) as the element concentration increased relative to the matrix (i.e. when moving from wet to oven dried to ashed samples). See Figure 4.2.2.

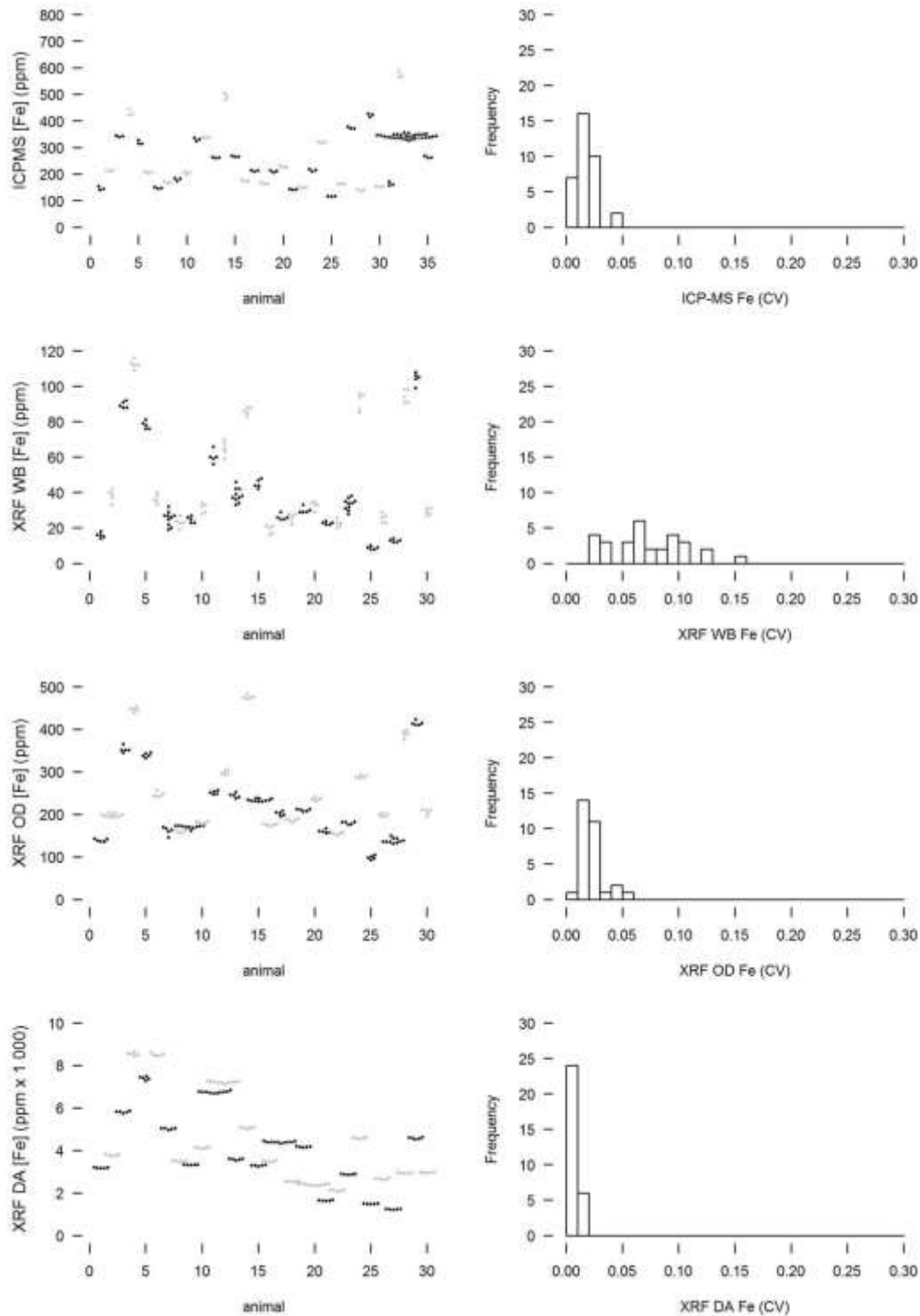


Figure 4.2.2 Fe concentrations as determined by ICP-MS and XRF.

4.2.3 MANGANESE

Mn was detectable using XRF spectrometry from a low concentration of 4.9 ppm oven-dried weight to a high of 272 ppm ashed weight, thus spanning at least 3 orders of magnitude. Mn was not detectable using XRF on wet samples. Precision of the XRF measurement (as indicated by intra-sample coefficient of variation) improved (CV decreased) as the element concentration increased relative to the matrix (i.e. when moving from oven-dried to ashed samples). See Figure 4.2.3.

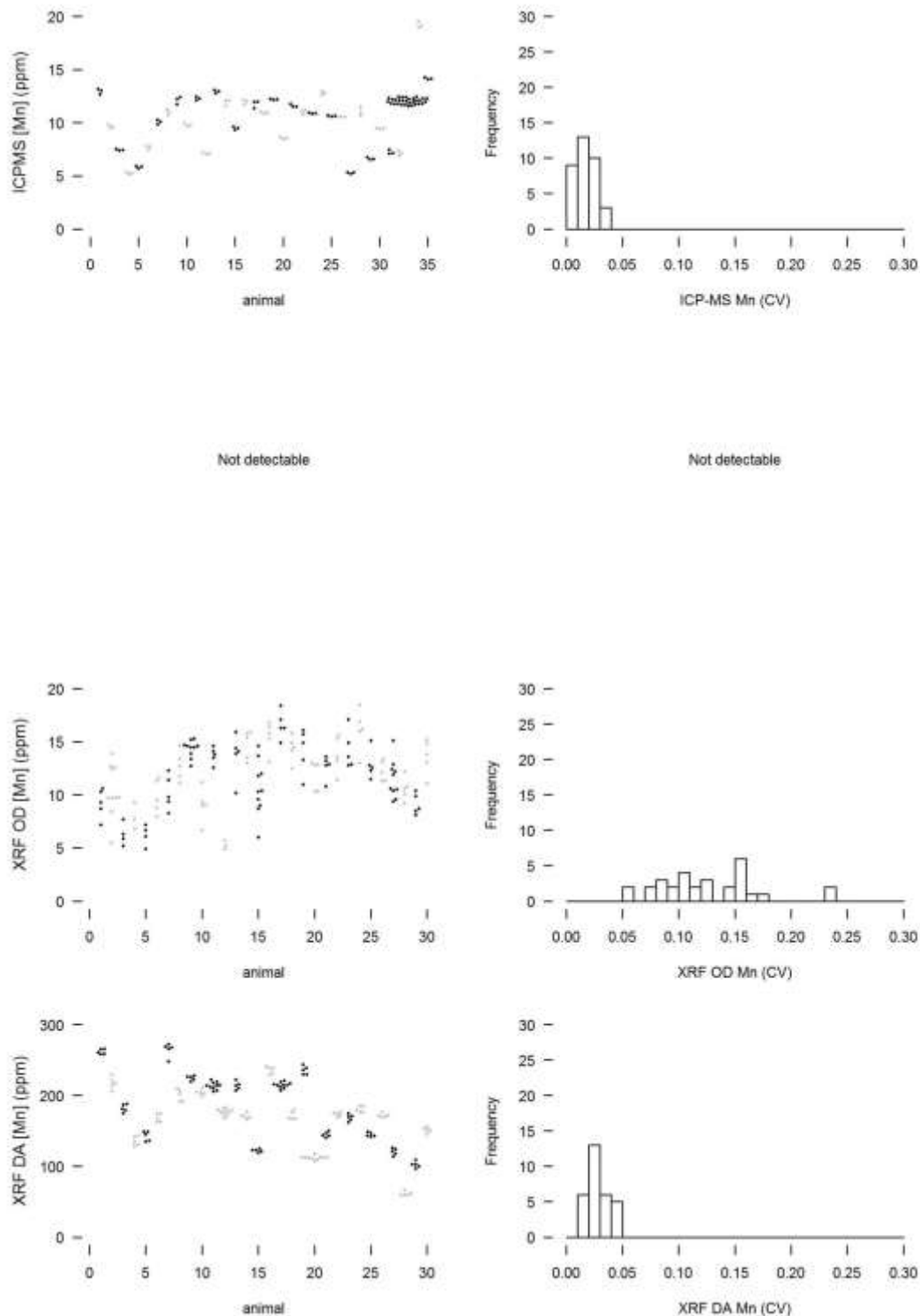


Figure 4.2.3 Mn concentrations as determined by ICP-MS and XRF.

4.2.4 MOLYBDENUM

Mo was detectable using XRF spectrometry from a low concentration of 1 ppm oven-dried weight to a high of 50 ppm ashed weight, thus spanning at least 2 orders of magnitude. Mo was not detectable using XRF on wet samples. Precision of the XRF measurement (as indicated by intra-sample coefficient of variation) improved (CV decreased) as the element concentration increased relative to the matrix (i.e. when moving from oven-dried to ashed samples). See Figure 4.2.4.

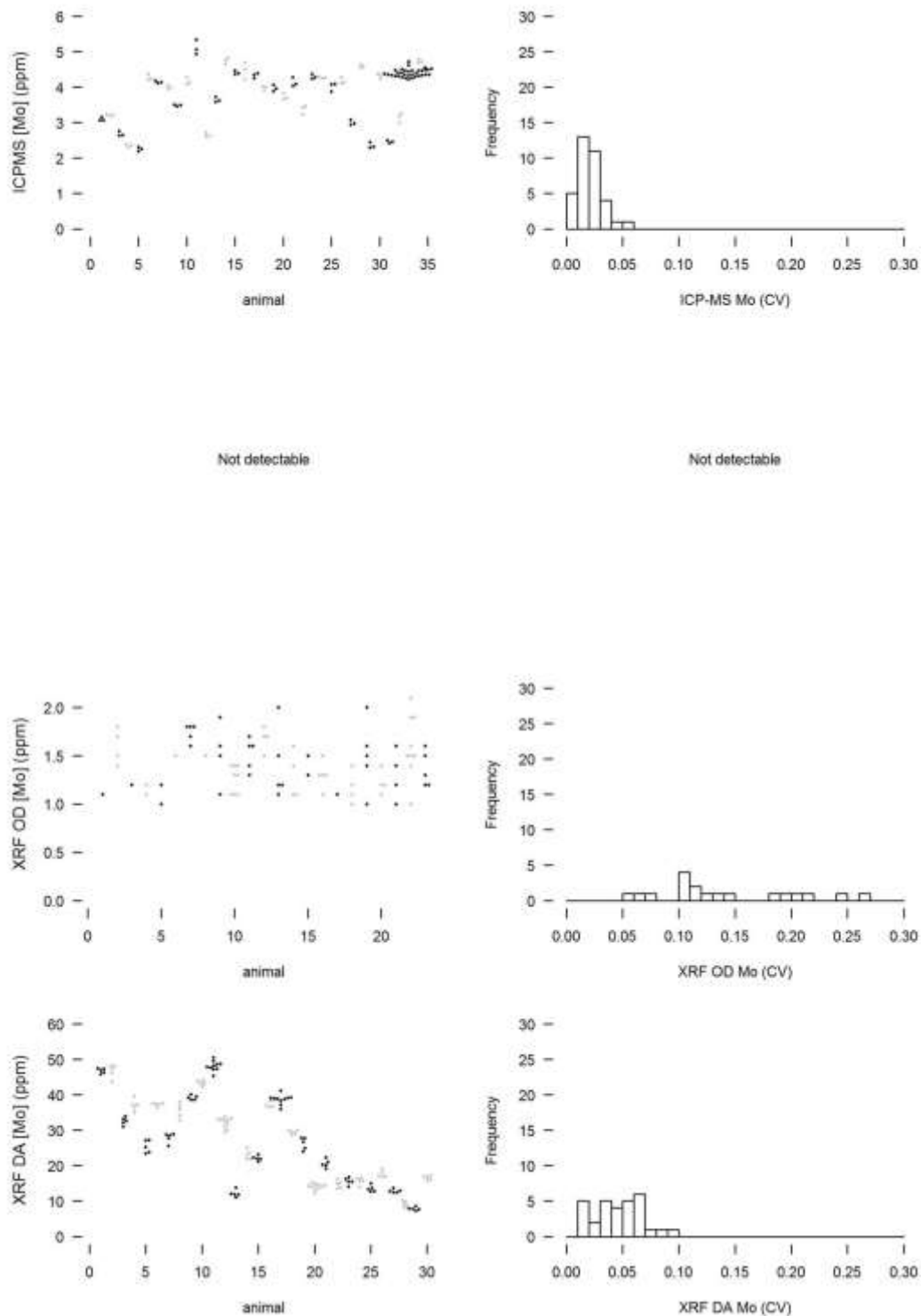


Figure 4.2.4 Mo concentrations as determined by ICP-MS and XRF.

4.2.5 SELENIUM

Se was detectable using XRF spectrometry from a low concentration of 1.6 ppm ashed weight to a high of 2.3 ppm ashed weight. Se was not detectable using XRF spectrometry on either wet or oven dried samples. See Figure 4.2.5.

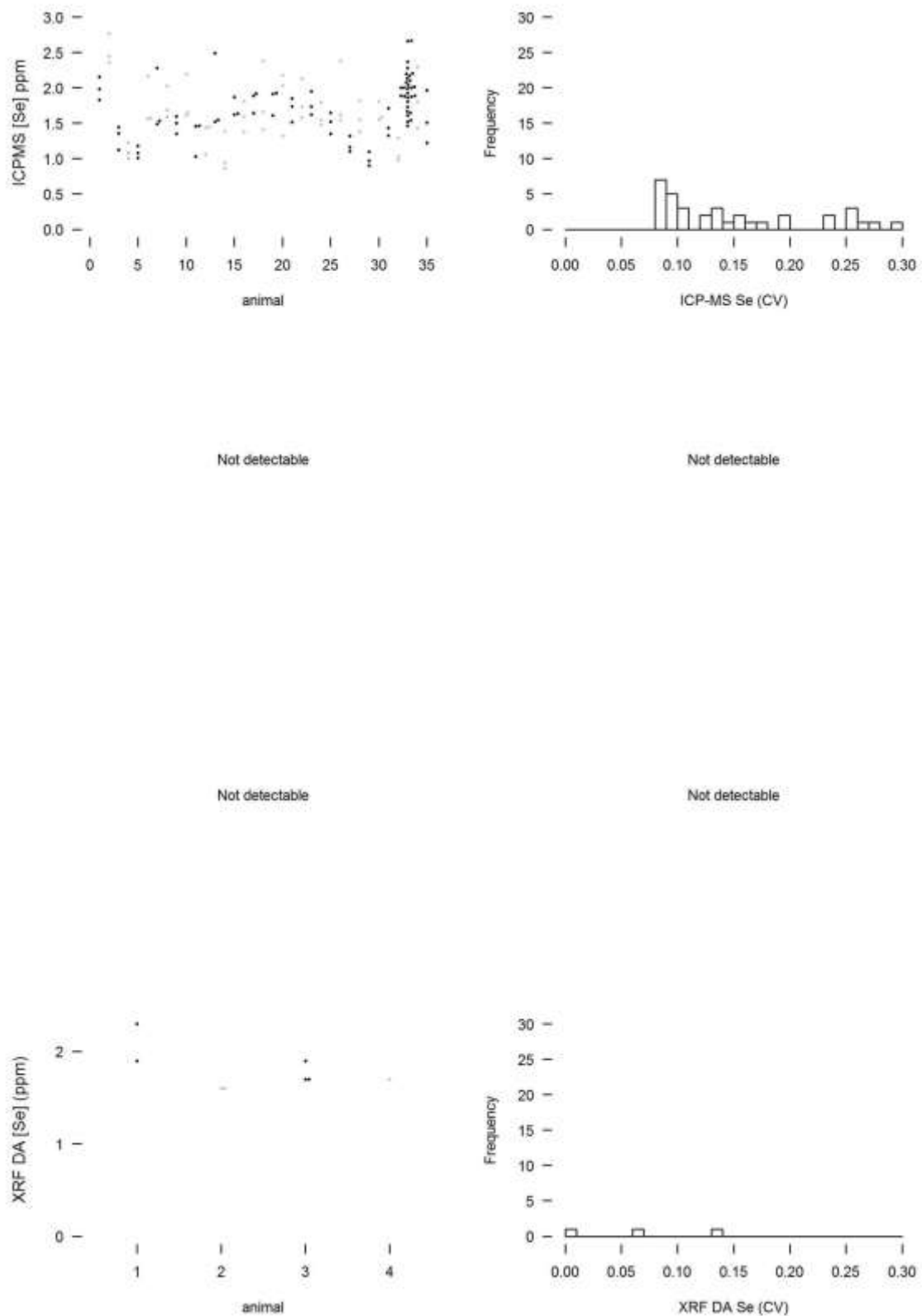


Figure 4.2.5 Se concentrations as determined by ICP-MS and XRF.

4.2.6 ZINC

Zn was detectable using XRF spectrometry from a low concentration of 25.7 ppm wet weight to a high of 3114 ppm ashed weight, thus spanning at least 3 orders of magnitude. Precision of the XRF measurement (as indicated by intra-sample coefficient of variation) improved (CV decreased) as the element concentration increased relative to the matrix (i.e. when moving from wet to oven-dried to ashed samples. See Figure 4.2.6.

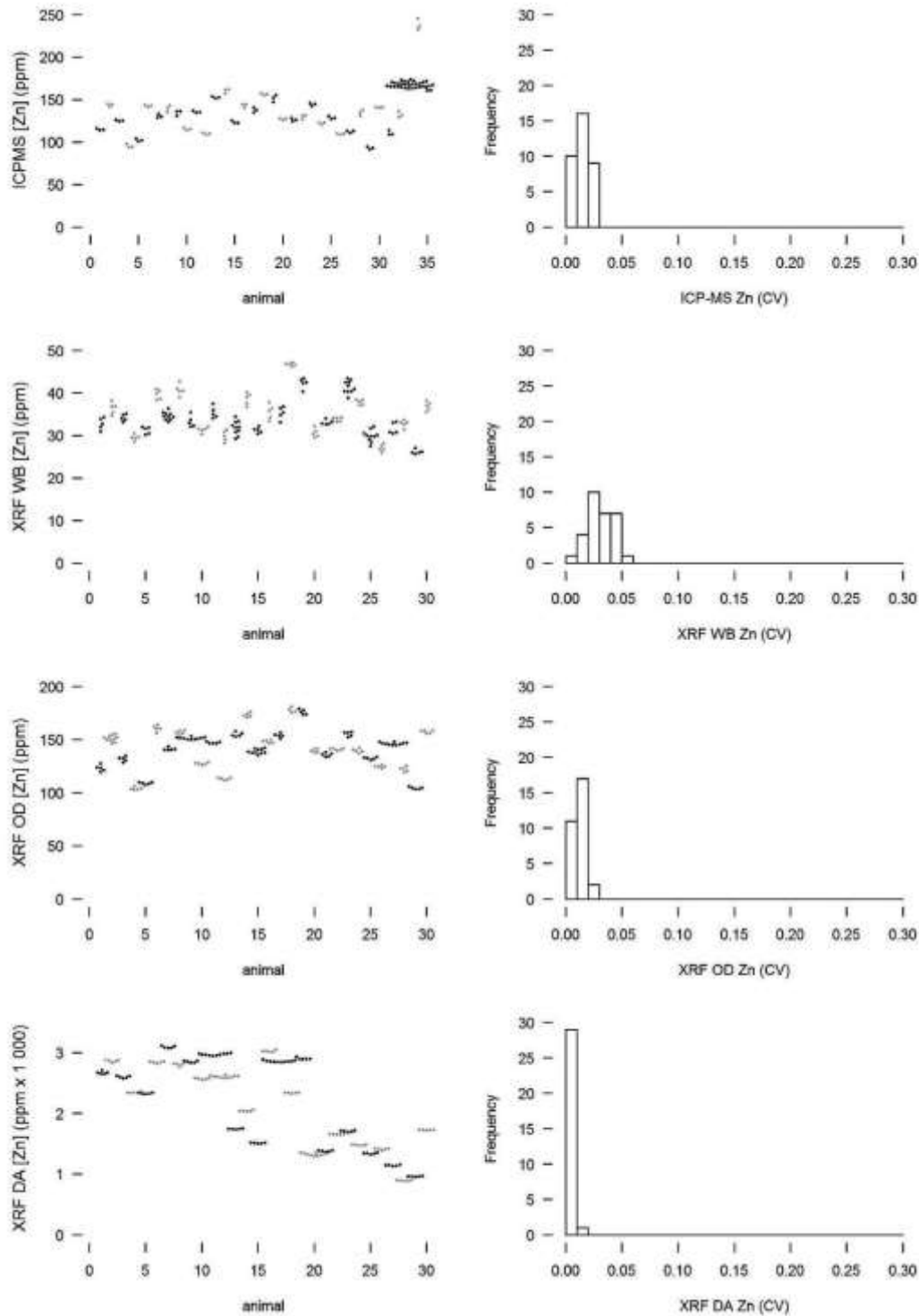


Figure 4.2.6 Zn concentrations as determined by ICP-MS and XRF.

The data in this study did not follow a normal distribution, but instead followed a log normal distribution. When data follows a log normal distribution, the median is used instead of the mean (Samuels & Witmer, 1999). The intra-sample coefficients of variation were similar between ICP-MS and XRF spectrometry when oven dried liver samples were analysed for Cu, Fe and Zn and were within the same order of magnitude for all elements when comparing ICP-MS to XRF spectrometry of the dry ashed liver samples. However, the intra-sample coefficients of variation for Mn and Mo were approximately an order of magnitude larger using XRF spectrometry. The precision for Se appears to be good when using XRF spectrometry on dry ashed liver samples. However, Se was only detected in a few samples, so this value is not representative of the overall precision of XRF spectrometry of dry ashed liver samples for Se content. Se was not detectable using XRF spectrometry for wet blended and oven dried liver samples. The intra-sample coefficient of variation for Se was relatively high using ICP-MS, suggesting that even the current 'gold standard' in detecting trace-elements may be imprecise in measuring Se. Overall, this suggests that the precision of analysis using XRF spectrometry is relatively good for Cu, Fe and Zn and relatively poor for Mn and Mo. Furthermore, XRF spectrometry cannot be reliably used for determining Se concentration.

Across all elements, moving from wet samples to oven-dried samples to ashed samples resulted in a relative increase in the concentration of the element, as water and then organic matter were removed. Due to the fact that Mn, Mo and Se were not detected in the wet blended samples, but Mn and Mo became detectable in the oven dried samples indicates that water molecules creates 'background noise' which interferes with the photons emitted by the XRF spectrometer resulting in less reliable results. The XRF spectrometry became more precise as these concentrations increased (lower intra-sample variability relative to a higher mean).

Table 4.2.1 ICP-MS median and range of intra-sample coefficient of variation (%) for element concentrations.

Element	Med	Min	Max
Cu	1.6	0.4	3.1
Fe	1.6	0.6	4.4
Mn	1.6	0.2	3.7
Mo	1.9	0.7	5.3
Se	13.5	8.0	29.8
Zn	1.3	0.4	3.0

Table 4.2.2 XRF median and range of intra-sample coefficient of variation (%) for element concentrations.

Element	Wet blend			Oven dried			Dry ashed		
	Med	Min	Max	Med	Min	Max	Med	Min	Max
Cu	1.7	0.8	5.6	0.7	0.1	1.7	0.5	0.2	1.4
Fe	6.8	2.0	15.9	2.0	0.9	5.8	0.8	0.5	1.6
Mn	-	-	-	12.1	5.4	23.9	2.6	1.4	4.9
Mo	-	-	-	12.1	5.1	26.2	4.7	1.3	9.6
Se	-	-	-	-	-	-	6.5	0.0	13.5
Zn	3.0	0.8	5.1	1.2	0.5	2.4	0.6	0.2	1.6

4.3 CORRELATIONS

Given the precision concerns, the median for each measurement, each element and each spectrometry method were used. All measurements that did not follow a normal distribution were log-transformed, as indicated. Sample preparation was specified for the XRF spectrometry as: wet blended (WB), oven-dried (OD), and dry ashed (DA). Bayesian correlation results were summarised by the median sample Pearson product-moment correlation coefficient (r), the 95% lower (LHPDI) and upper (UHPDI) highest posterior density intervals, the square of the sample correlation coefficient (r^2), and the probability that the correlation coefficient is positive. Frequentist correlation results were given as the correlation coefficient (r), the 95% lower (LCI) and upper (UCI) confidence interval, the square of the sample correlation coefficient (r^2), and the p -value (two-tailed probability of obtaining a result as extreme or more extreme than the observed data, given the null hypothesis ($H_0: r = 0$)).

In Figure 4.3.1 the correlations between Cu concentrations determined by XRF spectrometry after three different preparation methods (WB: wet blended, OD: oven-dried and DA: dry ashed) and determined by ICP-MS are indicated. The plots in the top half show the raw data (black dots) with ellipses covering 50 % and 95 % of the density of the estimated distribution. The raw data should fit the estimated distribution. The lower plots show the posterior distributions on the Pearson product-moment correlation coefficients (r , black curve) with the 95 % highest posterior density interval (HPDI: red line) with the median r (red dot).

For Cu, all measurement and preparation methods were positively correlated. These correlations were weak when the dry ashed preparation was compared to any other method. Relative to the 'gold standard' ICP-MS method, the oven-dried XRF method showed the strongest correlation (r closest to 1, with a very narrow highest posterior density interval around that value). Within the XRF spectrometry, the wet blended and oven-dried preparations had a strong positive correlation. The dry ashed preparation for XRF spectrometry had low or moderate positive correlations compared to other preparation methods.

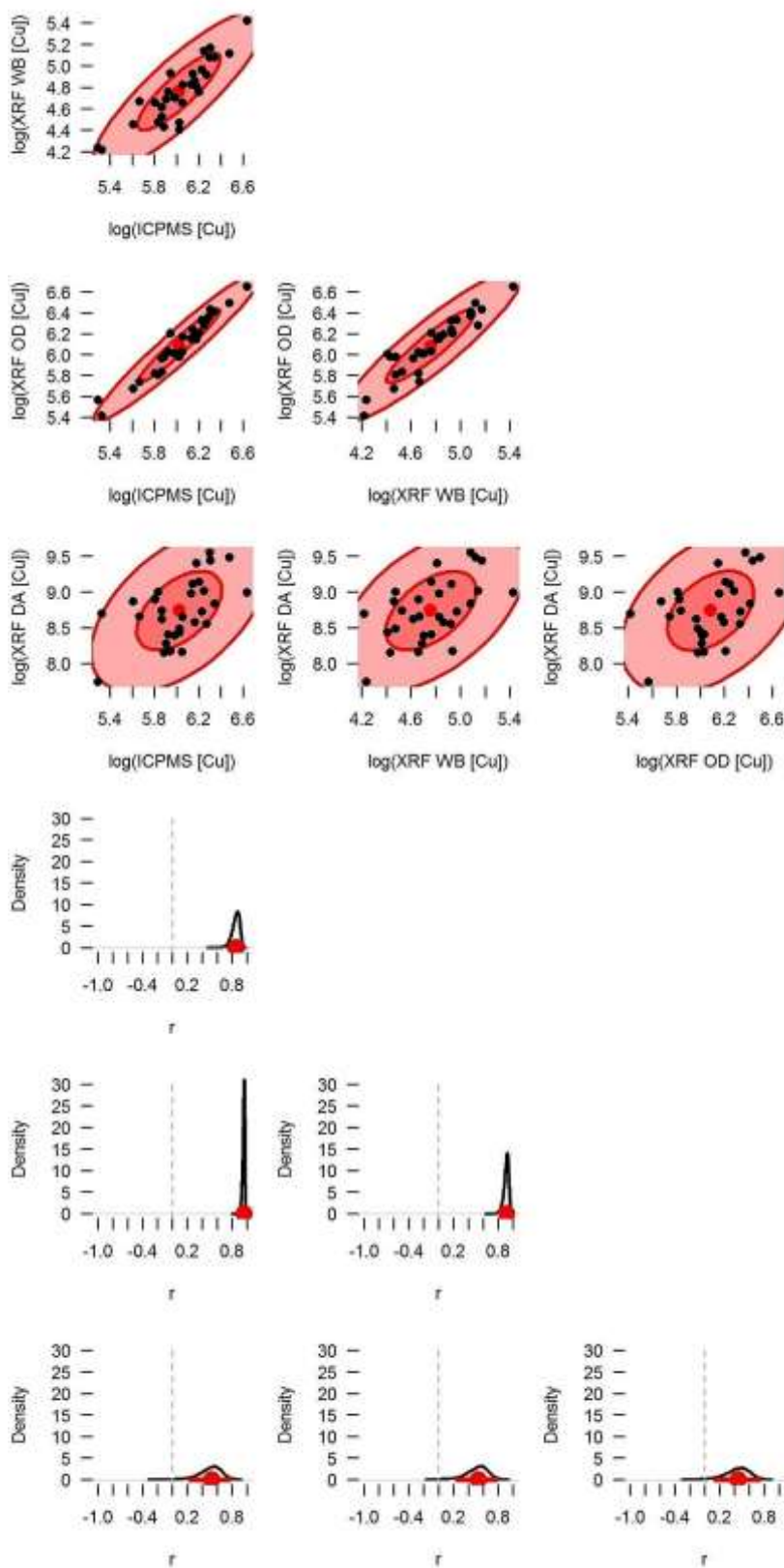


Figure 4.3.1 Correlations between Cu concentrations determined by XRF spectrometry and ICP-MS.

Figure 4.3.2 indicates correlations between Fe concentrations determined by XRF spectrometry after three different preparation methods (WB: wet blended, OD: oven-dried and DA: dry ashed) and determined by ICP-MS. The plots in the top half show the raw data (black dots) with ellipses covering 50 % and 95 % of the density of the estimated distribution. The raw data should fit the estimated distribution. The lower plots show the posterior distributions on the Pearson product-moment correlation coefficients (r , black curve) with the 95 % highest posterior density interval (HPDI: red line) with the median r (red dot).

For Fe, the wet blended and oven-dried XRF spectrometry indicated a strong positive correlation and both in turn showed a moderately strong positive correlation with the ICP-MS results. As with copper, the dry ashed preparation method indicated a moderate correlation with the ICP-MS data.

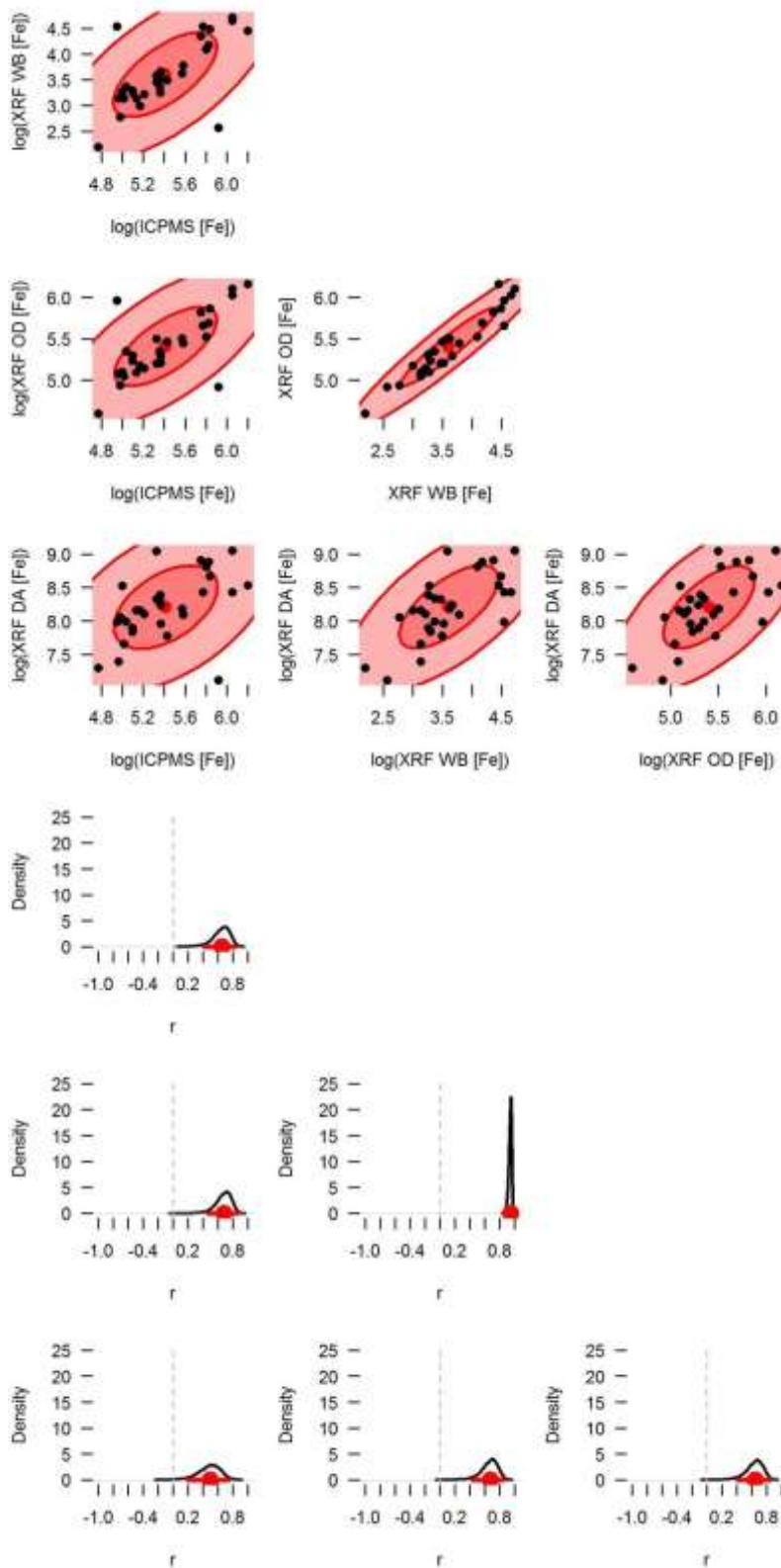


Figure 4.3.2 Correlations between Fe concentrations determined by XRF spectrometry and ICP-MS.

Figure 4.3.3 indicates correlations between Mn concentrations determined by XRF spectrometry after three different preparation methods (WB: wet blended, OD: oven-dried and DA: dry ashed) and determined by ICP-MS. The plots in the top half show the raw data (black dots) with ellipses covering 50 % and 95 % of the density of the estimated distribution. The raw data should fit the estimated distribution. The lower plots show the posterior distributions on the Pearson product-moment correlation coefficients (r , black curve) with the 95 % highest posterior density interval (HPDI: red line) with the median r (red dot).

Mn was not detectable using XRF spectrometry for the wet blended liver samples. The XRF spectrometry for the oven-dried preparation showed a moderately strong positive correlation with the ICP-MS data, while the XRF spectrometry for the dry ashed liver samples was weaker. There was no apparent association between the XRF spectrometry of oven-dried and dry ashed liver samples.

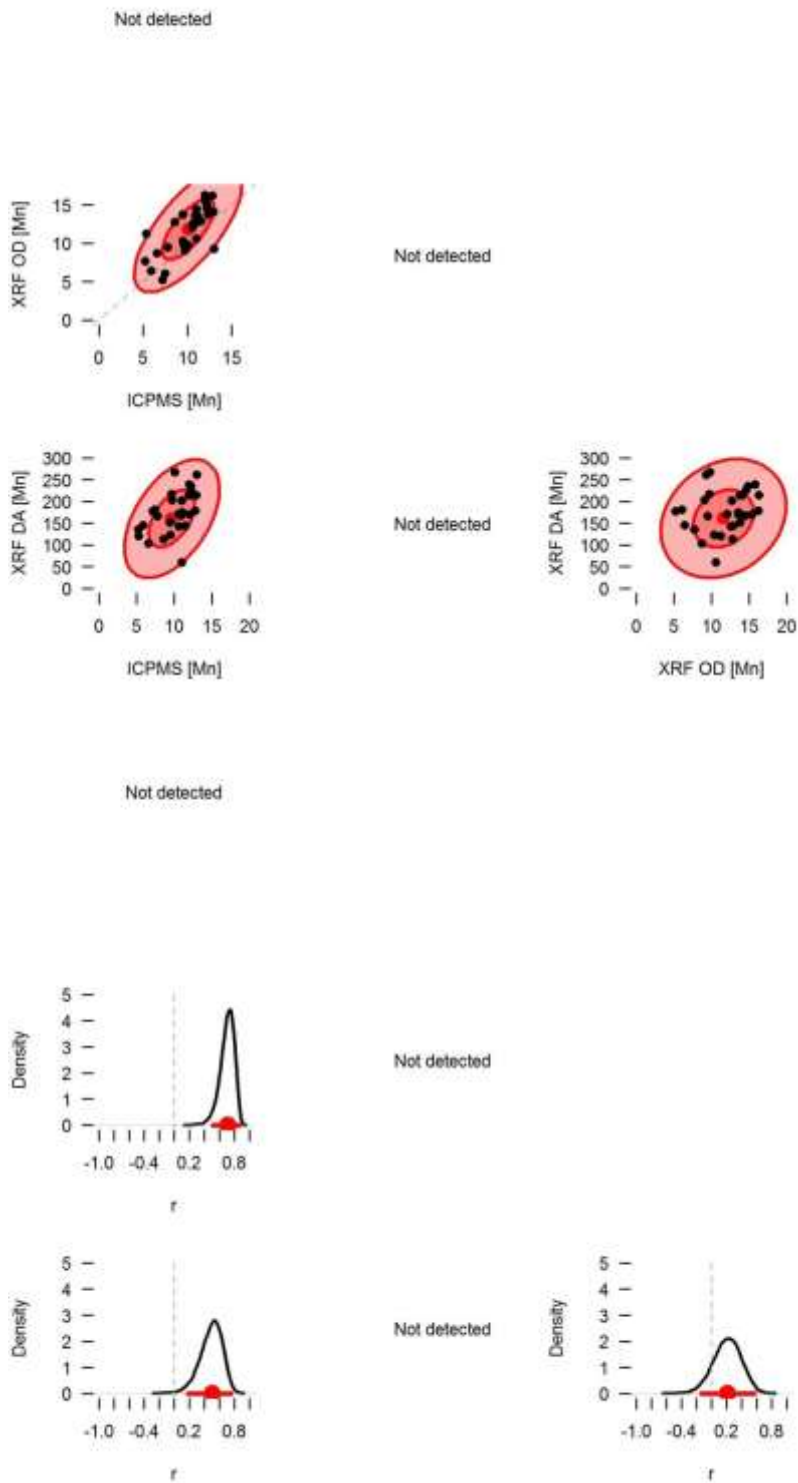


Figure 4.3.3 Correlations between Mn concentrations determined by XRF spectrometry and ICP-MS.

Figure 4.3.4 indicates correlations between Mo concentrations determined by XRF spectrometry after three different preparation methods (WB: wet blended, OD: oven-dried and DA: dry ashed) and determined by ICP-MS. The plots in the top half show the raw data (black dots) with ellipses covering 50 % and 95 % of the density of the estimated distribution. The raw data should fit the estimated distribution. The lower plots show the posterior distributions on the Pearson product-moment correlation coefficients (r , black curve) with the 95 % highest posterior density interval (HPDI: red line) with the median r (red dot).

For Mo, the XRF spectrometry of oven-dried liver samples indicated only a slight positive association with the ICP-MS data, while the XRF spectrometry of the dry ashed liver samples was not correlated with both the ICP-MS data and the XRF spectrometry concentrations of oven-dried liver samples.

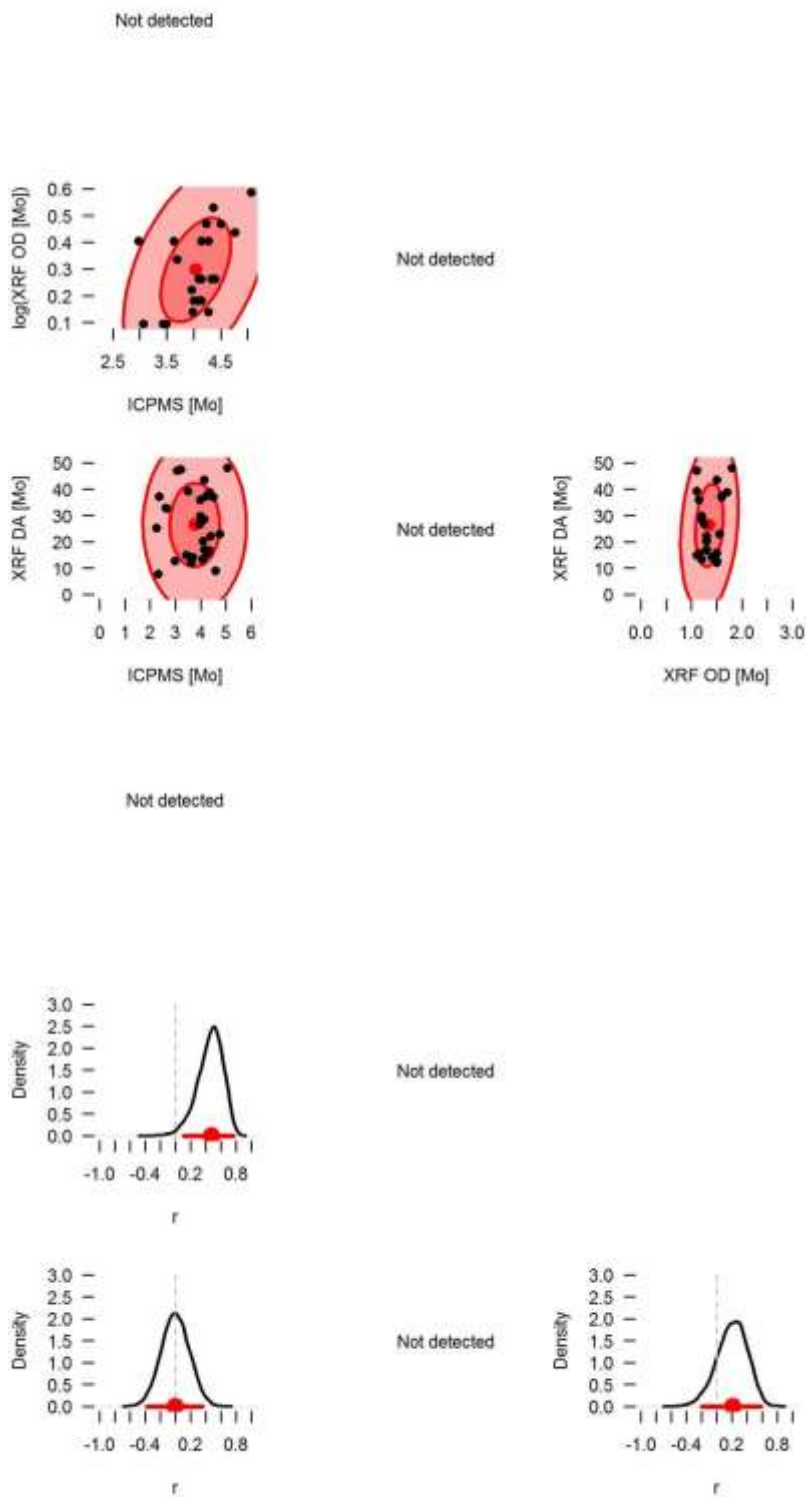


Figure 4.3.4 Correlations between Mo concentrations determined by XRF spectrometry and ICP-MS.

Figure 4.3.5 indicates correlations between Se concentrations determined by XRF spectrometry after three different preparation methods (WB: wet blended, OD: oven-dried and DA: dry ashed) and determined by ICP-MS. The plots in the top half show the raw data (black dots) with ellipses covering 50 % and 95 % of the density of the estimated distribution. The raw data should fit the estimated distribution. The lower plots show the posterior distributions on the Pearson product-moment correlation coefficients (r , black curve) with the 95 % highest posterior density interval (HPDI: red line) with the median r (red dot).

Se could only be detected using the dry ashed preparation with XRF spectrometry, and only in a few samples. With such a small sample size, no association was detected between the XRF spectrometry and ICP-MS data.

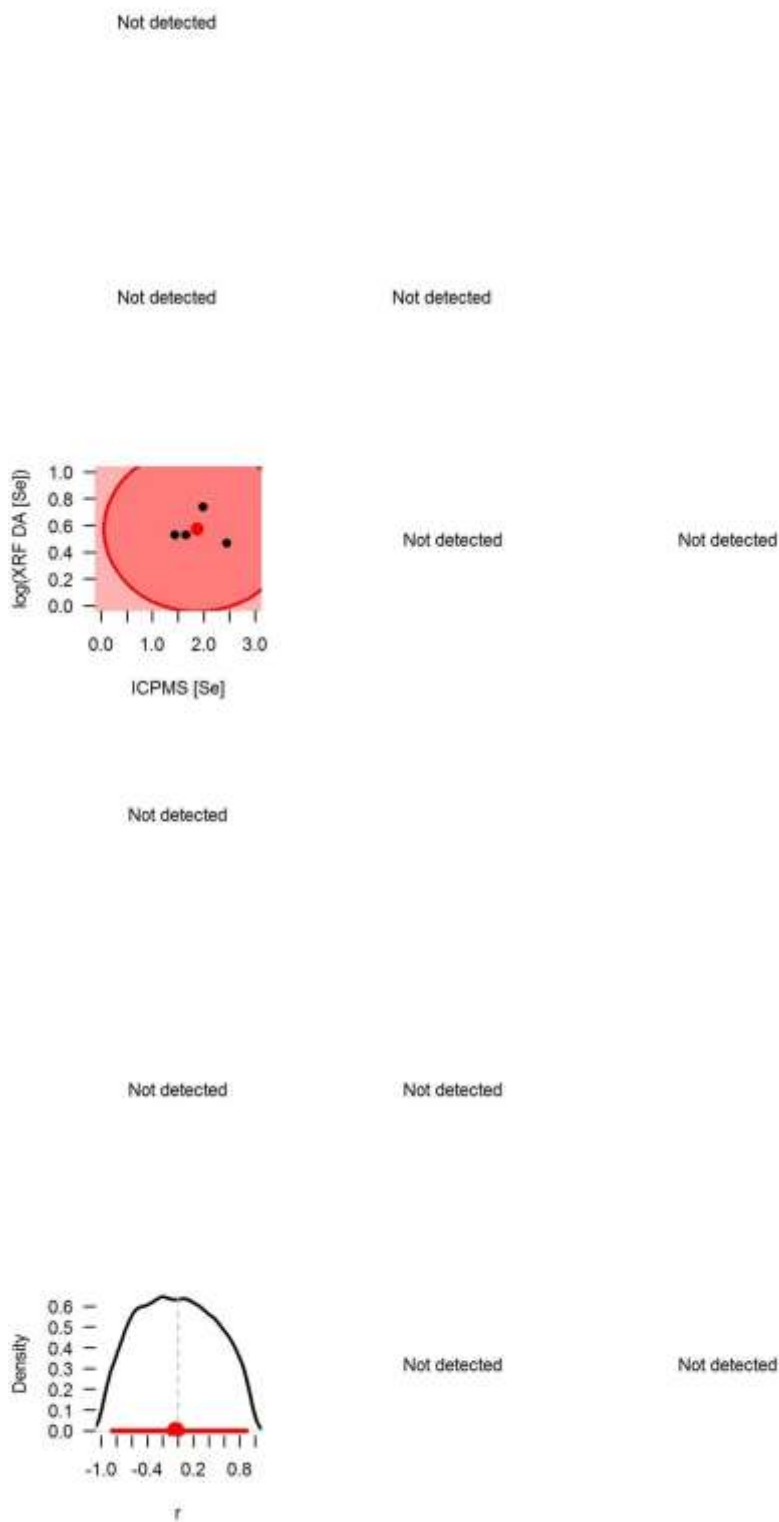


Figure 4.3.5 Correlations between Se concentrations determined by XRF spectrometry and ICP-MS.

Figure 4.3.6 indicates correlations between Zn concentrations determined by XRF spectrometry after three different preparation methods (WB: wet blended, OD: oven-dried and DA: dry ashed) and determined by ICP-MS. The plots in the top half show the raw data (black dots) with ellipses covering 50 % and 95 % of the density of the estimated distribution. The raw data should fit the estimated distribution. The lower plots show the posterior distributions on the Pearson product-moment correlation coefficients (r , black curve) with the 95 % highest posterior density interval (HPDI: red line) with the median r (red dot).

The best preparation to determine Zn concentration for XRF spectrometry was the oven-dried method. This preparation method exhibited the strongest positive correlation with ICP-MS. The wet blended analysis also showed a strong positive correlation with the ICP-MS as well as with the oven dried preparation method.

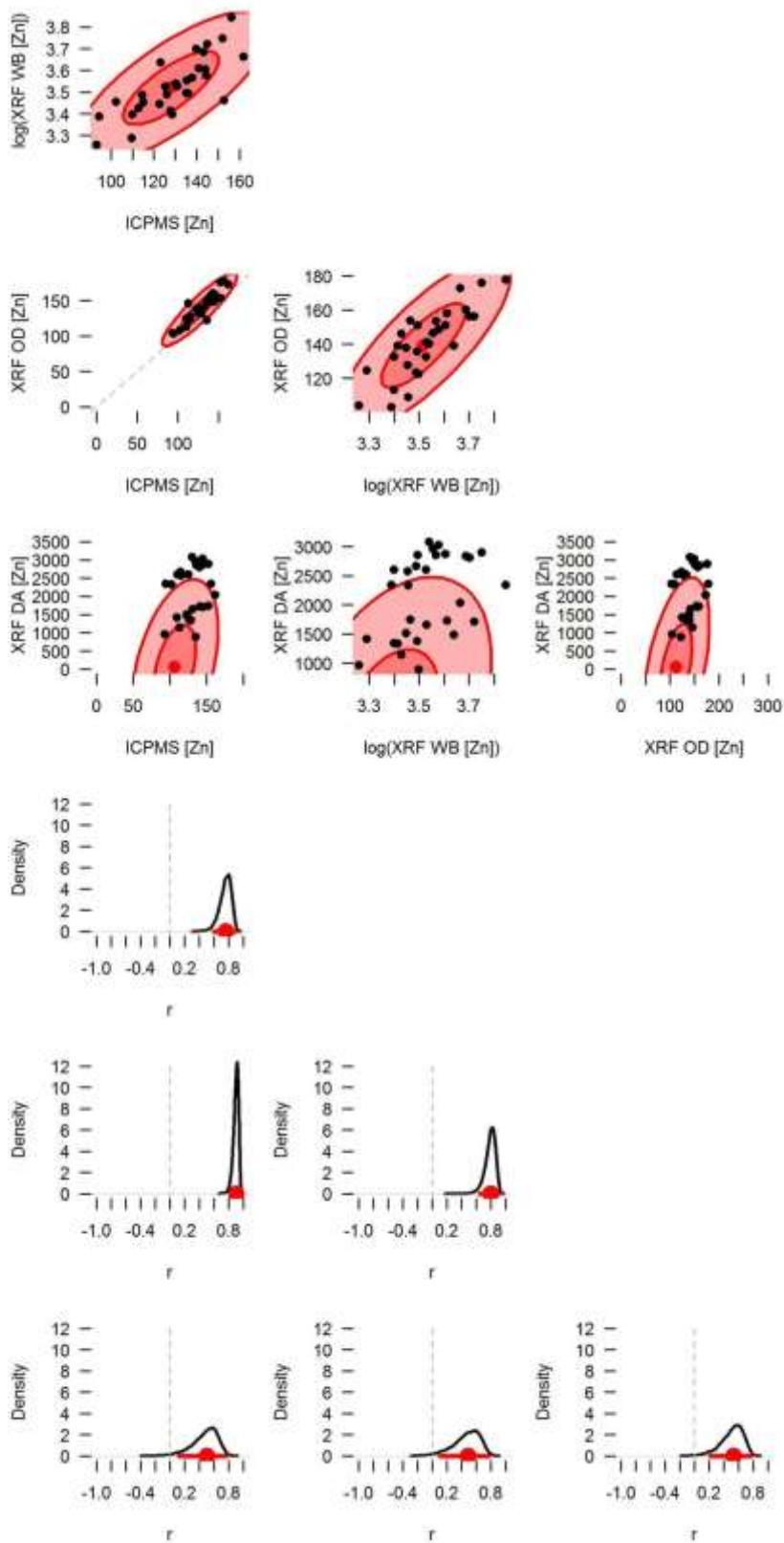


Figure 4.3.6 Correlations between Zn concentrations determined by XRF spectrometry and ICP-MS.

Volatilisation of certain elements during the ashing process may have contributed to the low or moderate positive correlations when comparing the results of the dry ashed prepared samples with the other preparation techniques (Prichard, MacKay & Points, 1996). Overall, the oven-dried preparation methods for XRF spectrometry appeared to provide the best correlation with the ICP-MS data. For Cu and Zn these correlations were strong, and handheld XRF spectrometry may represent a suitable substitute for analysis using ICP-MS. For Mn and Fe the correlations were moderately strong and XRF spectrometry may be suitable depending upon the intended application. For Mo the correlation was weak and XRF cannot be recommended. For Se no preparation method for XRF spectrometry was found suitable.

CHAPTER 5

CONCLUSIONS

The aim of this research project was to ascertain if the handheld XRF spectrometer will provide reliable concentrations of certain essential trace elements namely Cu, Fe, Mn, Mo, Se and Zn in the livers of sheep. Given the statistical analysis of the ICP-MS and handheld XRF spectrometry results, the precision of analysing ovine liver samples using handheld XRF spectrometry may be summarised as follows: relatively good for Cu, Fe and Zn, and relatively poor for Mn and Mo. Handheld XRF spectrometry cannot be reliably used for determining Se concentration in ovine livers.

When measuring concentrations of minerals present in samples at concentrations <5 ppm (e.g. Se) the handheld XRF methodology did not provide reliable results. Minerals present in samples at concentrations >5 ppm generally provided better and reliable results.

Comparing the wet blended, oven-dried and dry ashed preparation methods, the oven-dried preparations for handheld XRF spectrometry appeared to provide the strongest correlation with the ICP-MS (control) data. Correlations were relatively strong for Cu, Fe and Zn and handheld XRF spectrometry performed on oven-dried liver samples on these minerals is a suitable substitute for ICP-MS analysis. However, for Mo, the correlation was moderate and handheld XRF spectrometry cannot be recommended. Furthermore, analysis of liver samples using handheld XRF spectrometry to determine Se concentrations is also not suitable.

Further investigation with respect to the suitability of handheld XRF spectrometry for trace element analysis in diagnostic cases is strongly recommended. This may include the use of handheld XRF spectrometry to determine concentrations of certain minerals in other tissues such as kidney or bone as well.

The handheld XRF spectrometry may prove very reliable in determining concentrations of heavy metals such as Pb, Cd, Cr and even As in tissue samples of dead animals.

The handheld XRF spectrometer is easy to operate and due to its small size and light weight the handheld XRF spectrometer is portable.

An advantage is that it is not necessary to submit samples to a laboratory and the preparation and analysis can be performed at a clinic or local laboratory, thus limiting the cost of analysis. In addition, surveillance of mineral status of animals from various regions can be assessed at an abbatoir.

Another benefit of handheld X-ray fluorescence spectrometry is that the turnaround time of samples is greatly reduced. Instead of sending samples away for laboratory analysis and waiting for results, samples can be analysed more rapidly with the use of a handheld X-ray fluorescence spectrometer.

A disadvantage of the handheld X-ray fluorescence spectrometer is that the apparatus is expensive. It is therefore important to calculate the possible income to be made by obtaining a handheld X-ray fluorescence spectrometer to justify the purchase of such an apparatus.

REFERENCES

- Anonymous 2016, *Atomic absorption spectrometer block diagram*. Available: https://en.m.wikipedia.org/wiki/Atomic_absorption_spectroscopy [2016, June].
- Bath, G. & de Wet, J. 2000, *Sheep and Goat Diseases*, Tafelberg Publishers Limited, Cape Town.
- Beckhoff, B., Kanngiesser, B., Langhoff, N., Wedell, R. & Wolff, H. 2006, *Handbook of practical X-ray fluorescence analysis*, Springer, New York.
- Bellis, D.J., Todd, A.C. & Parsons, P.J. 2012, "An interlaboratory comparison of bone lead measurements via K-shell x-ray fluorescence spectrometry: validation against inductively coupled plasma mass spectrometry", *Journal of Analytical Atomic Spectrometry*, vol. 27, no. 4, pp. 595-603.
- Bezerra, M.A., Bruns, R.E. & Ferreira, S.L.C. 2006, "Statistical design-principal component analysis optimization of a multiple response procedure using cloud point extraction and simultaneous determination of metals by ICP OES", *Analytica Chimica Acta*, vol. 580, pp. 251-257.
- Bian, Q.Z., Jacob, P., Berndt, H. & Niemax, K. 2005, "Online flow digestion of biological and environmental samples for inductively coupled plasma-optical emission spectroscopy (ICP-OES)", *Analytica Chimica Acta*, vol. 538, pp. 323 – 329.
- Boss, C.B. & Fredeen, K.J. 2004, *Concepts, instrumentation and techniques in inductively coupled plasma optical emission spectrometry*, 3rd edn, PerkinElmer, Connecticut.
- Boyazoglu, P.A. 1973, "Mineral imbalances of ruminants in southern Africa", *South African Journal of Animal Science*, vol. 3, pp. 149 - 152.
- Bruker 2016, *X-ray diffraction and elemental analysis*. Available: www.bruker.com/products/x-ray-diffraction-and-elemental-analysis/handheld-xrf/how-xrf-works.html [2016, August].
- Carlson, B.A., Tobe, R., Yefremova, E., Tsuji, P.A., Hoffmann, V.J., Schweizer, U., Gladyshev, V.N., Hatfield, D.L. & Conrad, M. 2016, "Glutathione peroxidase 4 and vitamin E cooperatively prevent hepatocellular degeneration", *Redox Biology*, vol. 9, pp. 22 - 31.
- Committee on the nutrient requirements of small ruminants 2006, *Nutrient requirements of small ruminants: sheep, goats, cervids and new world camelids*, The National Academies Press, Washington, D.C.

- Commonwealth of Australia 2013, *X-rays*. Available: www.arpana.gov.au/radiationprotection/basics/x-rays.cfm [2016, August].
- Concordia College 2016, *Diagram of ICP-AES quartz torch compartment* [Homepage of Concordia College], [Online]. Available: sites.cord.edu/chem-330-lab-manual/experiments/icp-aes [2016, May].
- Dezfoulian, A.H., Aliarabi, H., Tabatabaei, M.M., Zamani, P., Alipour, D., Bahari, A. & Fadayifar, A. 2012, "Influence of different levels and sources of copper supplementation on performance, some blood parameters, nutrient digestibility and mineral levels in lambs", *Livestock Science*, vol. 147, no. 1, pp. 9-19.
- Ebbing, D.D. & Gammon, S.D. 1999, *General chemistry*, 6th edn, Houghton Mifflin, Boston MA.
- Ellis, A.T. 2002, "Energy-dispersive x-ray fluorescence analysis using x-ray tube excitation" in *Handbook of x-ray spectrometry*, eds. R.E. Van Grieken & A.A. Markowicz, 2nd edn, Marcel Dekker, Inc., pp. 199-236.
- Elsayed, M.E., Sharif, M.U. & Stack, A.G. 2016, "Transferrin saturation: a body iron biomarker", *Advances in Clinical Chemistry*, vol. 75, pp. 71 - 97.
- Erickson, A. 2015, *Copper deficiency in sheep and cattle* [Homepage of Government of Western Australia], [Online]. Available: <https://agric.wa.gov.au/n/3470> [2016, February].
- Erickson, A. 2015, *Selenium and/or vitamin E deficiencies in sheep* [Homepage of Government of Western Australia], [Online]. Available: <https://agric.wa.gov.au/n/2351> [2016, February].
- Eskina, V.V., Dalnova, O.A., Filatova, D.G., Baranovskaya, V.B. & Karpov, Y.A. 2016, "Separation and preconcentration of platinum-group metals from spent autocatalysts solutions using a hetero-polymeric S,N-containing sorbent and determination by high-resolution continuum source graphite furnace atomic absorption spectrometry", *Talanta*, vol. 159, pp. 103 - 110.
- Fuwa, K. 1999, "Memories of Sir Alan Walsh: atomic absorption spectroscopy in the field of trace elements in biology", *Spectrochimica Acta Part B: Atomic spectroscopy*, vol. 54, no. 14, pp. 2005 - 2009.
- Gartner, A. & Weser, U. 1983, "Erythrocyte is the major copper protein of the red blood cell", *FEBS Letters*, vol. 155, no. 1, pp. 15 -18.
- Giancoli, D.C. 1998, *Physics*, 5th edn, Prentice Hall, New Jersey.
- Goodrich, R.D. & Tillman, A.D. 1966, "Copper, sulfate and molybdenum interrelationships in sheep", *Journal of Nutrition*, vol. 90, no. 1, pp. 76 - 80.

- Helsen, J.A. & Kuczumow, A. 2002, "Wavelength-dispersive x-ray fluorescence" in *Handbook of x-ray spectrometry*, eds. R.E. Van Grieken & A.A. Markowicz, 2nd edn, Marcel Dekker, Inc., pp. 95-191.
- Hogan, K.G., Money, D.F.L. & Walker, R.S. 1971, "The distribution of copper in the liver of pigs and sheep and its effect on the value of chemical analysis made on biopsy samples", *New Zealand Journal of Agricultural Research*, vol. 14, pp. 132 – 141.
- Hoon, J.H. & Herselman, M.J. 2007, "Trace mineral supplementation of sheep and angora goats in the different grazing areas of South Africa", *Grootfontein Agric*, vol. 7, no. 1, pp. 7-13.
- Iyengar, G.V. 1989, *Elemental analysis of biological systems*, CRC Press, Florida.
- Jenkins, R. 1999, *X-ray fluorescence spectrometry*, 2nd edn, John Wiley & Sons, Inc., New York.
- Kahn, B.A. 2005, *The Merck veterinary manual*, 9th edn, Merck & Co, Inc., New Jersey.
- Kairtyahann, S.R. 1980, "A history of atomic absorption spectroscopy", *Spectrochimica Acta Part B: Atomic spectroscopy*, vol. 35, no. 11 - 12, pp. 663 -670.
- Kryazhov, A., Panova, S., Kolpakova, N. & Pshenichkin, A. 2014, "Determination of Au, Pb, Ni and Co in mineral raw materials by atomic absorption spectroscopy with graphite furnace", *Procedia Chemistry*, vol. 10, pp. 437-440.
- Larson, C.K. 2005, *Role of trace minerals in animal production*. Available: <http://www.animalrange.montana.edu/documents/courses/ANSC320/ConnieLarsenTraceMinerals.pdf> [2016, February].
- Mader, S.S. 2001, *Biology*, 7th edn, McGraw-Hill, New York.
- McC Howell, J. 1996, "Toxicities and excessive intakes of minerals" in *Detection and treatment of mineral nutrition problems in grazing sheep*, eds. D.G. Masters & C.L. White, Australian Center for International Agricultural Research, , pp. 95-117.
- McDonald, P., Edwards, R.A., Greenhalgh, J.F.D. & Morgan, C.A. 2002, *Animal nutrition*, 6th edn, Pearson Prentice Hall, Harlow, England.
- Menzies, P.I., Boermans, H., Hoff, B. & Durzi, T. & Langs, L. 2003, "Survey of copper, interacting minerals, and vitamin E levels in the livers of sheep in Ontario", *The Canadian Veterinary Journal*, vol. 44, no. 11, pp. 898 - 906.

- Morton, A.G. & Tavill, A.S. 1977, "The role of iron in the regulation of hepatic transferrin synthesis", *British Journal of Haematology*, vol. 36, no. 3, pp. 383 - 394.
- Nganvongpanit, K., Buddhachat, K., Klinhom, S., Kaewmong, P., Thitaram, C. & Mahakkanukrauh, P. 2016, "Determining comparative elemental profile using handheld X-ray fluorescence in humans, elephants, dogs and dolphins", *Forensic Science International*, vol. 263, pp. 101 - 106.
- Nomura, C.S., Silva, C.S., Nogueira, A.R.A. & Oliveira, P.V. 2005, "Bovine liver sample preparation and micro-homogeneity study for Cu and Zn determination by solid sampling electrothermal atomic absorption spectrometry", *Spectrochimica Acta Part B: Atomic spectroscopy*, vol. 60, no. 5, pp. 673 - 680.
- Oxford instruments 2016, *High performance, multisample benchtop XRF analyser-x-supreme 8000*. Available: www.oxford-instruments.com/products/analysers/stationary-benchtop-analyser/x-supreme8000 [2016, August].
- Prichard, E., MacKay, G.M. & Points, J. 1996, *Trace analysis: A structured approach to obtaining reliable results*, The Royal Society of Chemistry, United Kingdom, pp. 68 – 71.
- Puls, R. 1994, *Mineral levels in animal health: Diagnostic data*, 2nd edn, Sherpa International, Clearbrook, Canada.
- Reis, L.S., Pardo, P.E. & Camargos, A.S. & Oba, E. 2010, "Mineral element and heavy metal poisonings in animals", *Journal of Medicine and Medical Sciences*, vol. 1, no. 12, pp. 560 - 579.
- Roberts, E.A. & Sarkor, B. 2008, "Liver as a key organ in the supply, storage and excretion of copper", *American Journal of Clinical Nutrition*, vol. 88, no. 3, pp. 851 - 854.
- Robinson, J.W. 1996, *Atomic spectroscopy*, 2nd edn, Marcel Dekker Inc., New York.
- Samuels, M.L. & Witmer, J.A. 1999, *Statistics for the life sciences*, 2nd edn, Prentice-Hall, New Jersey.
- Sansinanea, A.S., Cerone, S.I., Elperding, A. & Nestor, A. 1996, "Glucose-6-phosphate dehydrogenase activity in erythrocytes from chronically copper-poisoned sheep", *Comparative Biochemistry and Physiology Part C; Pharmacology, Toxicology and Endocrinology*, vol. 114, no. 3, pp. 197 - 200.

- Swenson, J.M. & Reece, W.O. 1993, *Dukes' physiology of domestic animals*, 11th edn, Cornell University Press, New York.
- Takahashi, S., Takahashi, I., Sato, H., Kubato, Y., Yoshida, S. & Muramatsu, Y. 2000, "Determination of major and trace elements in the liver of Wistar rats by inductively coupled plasma-atomic emission spectrometry and mass spectrometry", *Laboratory Animals*, vol. 34, pp. 97 - 105.
- Thermo-Scientific. 2016, 2016-last update, *How xrf works*. Available: in.niton.com/en/portable-xrf-technology/how-xrf-works [2016, 13-3-2016].
- Thomas, R. 2013, *Practical guide to ICP-MS: A tutorial for beginners*, 3rd edn, CRC Press, Florida.
- Thomas, R. 2004, *Practical guide to ICP-MS*, Marcel Dekker, Inc., New York.
- Thrall, D.E. 2002, *Textbook of veterinary diagnostic radiology*, 4th edn, Saunders, Pennsylvania.
- Underwood, E.J. & Shuttle, N.F. 1999, *The mineral nutrition of livestock*, 3rd edn, CABI, Wallingford, England.
- Van Doren, C. 2015, 4-1-2015-last update, *Trace element* [Homepage of Encyclopaedia Britannica, Inc.], [Online]. Available: <http://www.britannica.com/science/trace-element> [2016, 1-2-2016].
- Van Ryssen, J.B.J. 2001, "Geographical distribution of the selenium status of herbivores in South Africa", *South African Journal of Animal Science*, vol. 31, no. 1, pp. 1 - 7.
- Vatn, S. & Framstad, T. 2000, "Anaemia in housed lambs: effects of oral iron on clinical pathology and performance", *Acta veterinaria Scandinavica*, vol. 41, pp. 273 - 281.
- Walsh, A. 1989, "The application of atomic absorption spectra to chemical analysis", *Spectrochimica Acta Part A: Molecular spectroscopy*, vol. 45, pp. 221 - 230.
- Wang, T. 2004, "Inductively coupled plasma optical emission spectrometry" in *Analytical Instrumentation Handbook*, ed. J. Cazes, 3rd edn, CRC Press, Florida, pp. 57 - 74.
- Warren, M. & Smith, A. 2009, *Tetrapyrroles: Birth, life and death*, Springer Science & Business media, New York.
- Wolf, R.E. 2013, , *What is ICP-MS?*. Available: crustal.usgs.gov/laboratories.icpms/intro.html [2016, June].

Zhang, C., Bruins, M.E., Yang, Z., Liu, S. & Rao, P. 2016, "A new formula to calculate activity of superoxide dismutase in indirect assays", *Analytical Biochemistry*, vol. 503, pp. 65 - 67.

Zimmerman, H.A. 2013, *Preliminary validation of handheld x-ray fluorescence (HHXRF) spectrometry: distinguishing osseous and dental tissue from non-bone material of similar chemical composition*, University of Central Florida.

APPENDUM A



UNIVERSITEIT VAN PRETORIA
UNIVERSITY OF PRETORIA
YUNIBESITHI YA PRETORIA

Animal Ethics Committee

PROJECT TITLE	Important trace element concentrations in ovine liver as determined by energy dispersive handheld x-ray fluorescence spectrometry
PROJECT NUMBER	V087-16
RESEARCHER/PRINCIPAL INVESTIGATOR	Dr. DE van Loggerenberg

STUDENT NUMBER (where applicable)	UP_96139839
DISSERTATION/THESIS SUBMITTED FOR	MSc

ANIMAL SPECIES	n/a	
NUMBER OF ANIMALS	n/a	
Approval period to use animals for research/testing purposes	August 2016 – August 2017	
SUPERVISOR	Prof. CJ Botha	

KINDLY NOTE:

Should there be a change in the species or number of animal/s required, or the experimental procedure/s - please submit an amendment form to the UP Animal Ethics Committee for approval before commencing with the experiment

APPROVED	Date	29 August 2016
CHAIRMAN: UP Animal Ethics Committee	Signature	